nature medicine

Supplementary information

https://doi.org/10.1038/s41591-025-03719-2

Individual variations in glycemic responses to carbohydrates and underlying metabolic physiology

In the format provided by the authors and unedited

Supplementary Methods

Metabolomics and lipidomics sample preparation

Metabolites and complex lipids were extracted using a biphasic separation with cold methyl tert-butyl ether (MTBE), methanol, and water in the deep well plate format. Briefly, 1ml of ice-cold MTBE and 260µl methanol were added to 40µl of the plasma spiked-in with 40µl deuterated lipid internal standards (Sciex, cat# 5040156, lot# LPISTDKIT-103). The samples were then agitated at 4°C for 30 minutes. After the addition of 250µl of ice-cold water, the samples were vortexed for 1 minute and centrifuged at 3,800 g for five minutes at 4°C. The upper organic phase contained the lipids, the lower aqueous phase contained the metabolites, and the proteins were precipitated at the bottom of the well. For quality control, three reference plasma samples (40µl plasma) as well as one control sample lacking any sample were processed in parallel per plate.

For metabolomics samples, proteins were further precipitated by adding 500µl of 1:1:1 acetone:acetonitrile:methanol spiked-in with 15 labeled metabolite internal standards to 300µl of the aqueous phase and 200µl of the lipid phase and incubating the samples overnight at -20°C. After centrifugation at 3,800 g for 10 minutes at 4°C, the metabolic extracts were dried down to completion and resuspended in 200µl 50/50 methanol/water for liquid chromatography–mass spectrometry (LC-MS) analysis.

For lipidomics, 700µl of the organic phase was dried down under a stream of nitrogen and resolubilized in 200µl of methanol for storage at -20°C until analysis. On the day of the analysis, samples were dried down, resuspended in 300µl of 10mM ammonium acetate in 90:10 methanol:toluene and centrifuged at 3,800 g for five minutes at 4°C.

Metabolomics data acquisition and processing

Metabolite extracts were analyzed using a broad-spectrum untargeted LC-MS platform[56]. Metabolic extracts were analyzed four times using hydrophilic interaction liquid chromatography (HILIC) and reverse phase liquid chromatography (RPLC) separation in both positive and negative ionization modes. Data were acquired on a Thermo Q Exactive HF mass spectrometer for HILIC (Thermo Fisher Scientific, Bremen, Germany) and a Thermo Q Exactive mass spectrometer for RPLC (Thermo Fisher Scientific, Bremen, Germany). Both instruments were equipped with a HESI-II probe and operated in full MS scan mode. MS/MS data were acquired on quality control samples (QC) consisting of an equimolar mixture of all samples in the study. HILIC experiments were performed using a ZIC-HILIC column 2.1 x 100mm, 3.5µm, 200Å (Merck Millipore, Darmstadt, Germany) and mobile phase solvents consisting of 10mM ammonium acetate in 50/50 acetonitrile/water (A) and 10 mM ammonium acetate in 95/5 acetonitrile/water (B). RPLC experiments were performed using a Zorbax SBaq column 2.1 x 50mm, 1.7µm, 100Å (Agilent Technologies, Palo Alto, CA) and mobile phase solvents consisting of 0.06% acetic acid in water (A) and 0.06% acetic acid in methanol (B). Data quality was ensured by (i) injecting 6 and 12 pool samples to equilibrate the LC-MS system prior to running the sequence for RPLC and HILIC, respectively, (ii) injecting a pool sample every 10 injections to control for signal deviation with time, and (iii) checking mass accuracy, retention time and peak shape of internal standards in each sample.

Data from each mode were independently analyzed using Progenesis QI software (v2.3) (Nonlinear Dynamics, Durham, NC). Metabolic features from blanks and those that did not show sufficient linearity upon dilution in QC samples ($r<0.6$) were discarded. Only metabolic features present in >2/3 of the samples were kept for further analysis. Missing values were imputed by drawing from a random distribution of low values in the corresponding sample. Intensity drift was corrected using the SERRF (systematic error removal using random forest) method[57]. Data from each mode were merged and metabolic features were annotated as follows. Peak annotation was first performed by matching experimental m/z, retention time, and MS/MS spectra to an in-house library of analytical-grade standards. The remaining peaks were identified by matching experimental m/z and fragmentation spectra to publicly available databases including Human Metabolome Database (HMDB), MassBank of North America (MoNA), MassBank, METLIN, and NIST using the R package 'metID' (v0.2.0) [55]. We used the Metabolomics Standards Initiative (MSI) level of confidence to grade metabolite annotation confidence (level 1 - level 3). Level 1 represents formal identifications where the biological signal matches accurate mass, retention time, and fragmentation spectra of an authentic standard run on the same platform. For level 2 identification, the biological signal matches accurate mass and fragmentation spectra available in one of the public databases listed above. Level 3 represents putative identifications that are the most likely names based on previous knowledge.

Lipidomics data acquisition and processing

Complex lipids were quantified using a targeted MS-based approach[58]. *Targeted Lipidomics using the Lipidyzer Platform.* Lipid extracts were analyzed using the Lipidyzer platform that comprises a 5500 QTRAP system equipped with a SelexION differential mobility spectrometry (DMS) interface (Sciex) and a high flow LC-30AD solvent delivery unit (Shimazdu, Columbia, MD). Briefly, lipid molecular species were identified and quantified using multiple reaction monitoring (MRM) and positive/negative ionization switching. Two acquisition methods were employed covering 13 lipid classes; method 1 had SelexION voltages turned on while method 2 had SelexION voltages turned off. Data quality was ensured by i) tuning the DMS compensation voltages using a set of lipid standards (cat# 5040141, Sciex) after each cleaning, more than 24 hours of idling or three days of consecutive use, ii) performing a quick system suitability test (QSST) (cat# 5040407, Sciex) before each batch to ensure acceptable limit of detection for each lipid class, and iii) triplicate injection of lipids extracted from a reference plasma sample (cat# 4386703, Sciex) at the beginning of the batch.

Lipidyzer data were reported by the Lipidomics Workflow Manager (LWM, v1.0.5.0) software which calculates concentrations for each detected lipid as the average intensity of the analyte MRM divided by the average intensity of the most structurally similar internal standard (IS) MRM multiplied by its concentration. Lipids detected in less than 2/3 of the samples were discarded and missing values were imputed by drawing from a random distribution of low values class-wise in the corresponding sample. Lipid abundances were reported as concentrations in nmol/g.

Proteomics collection and processing

Proteomics data was measured by using the Olink Explore 1536 panel from plasma samples and normalized as Normalized Protein eXpression (NPX). Proximity extension antibody assays were used to quantify protein expression levels. Quality control was performed by identifying outliers within each protein panel by principal component analysis and by assessment of median and interquartile range values for normalized NPX across protein samples. This analysis was performed using the OlinkAnalyze package in R, which was developed and maintained by the Olink Proteomics Data Science Team.

Microbiome collection and processing

Raw stool samples were collected in 50mL tubes and frozen immediately in -80°C freezers until sample processing. For processing, samples were removed from the freezer and placed on dry ice to keep frozen, and aliquoted using Miltex 5mm Biopsy Punches to obtain uniform sample sizes from frozen stools. Every stool aliquot was weighed to the mg prior to adding to bead beating tubes and reagents from the Zymo Research Zymobiomics 96 DNA Extraction Kit. The Zymo bead beating solution was spiked in a master mix per 96-well plate with two aliquots of the Zymobiomics Spike-In Control I High Microbial Load to allow for absolute abundance normalization when reads were adjusted by sample weight. Bead beating was performed using an OMNI International Bead Ruptor 96 Well Plate Homogenizer for three minutes at a frequency of 30 beats per second. The standard extraction Zymobiomics 96 DNA Extraction protocol was performed using provided reagents and an Eppendorf epMotion 96 well pipetting system for uniform and consistent liquid handling. DNA quantification was assessed by fluorescence on a Molecular Devices SpectraMax ID3 using the SpectraMax Quant Accuclear Nano DS DNA Kit. DNA was aliquoted into plates for library preparation and sequencing based on cutoffs of <2ng/uL for low concentration and 2-10ng/uL for high concentration library preparation, with samples of >10ng/uL concentration being diluted to the 2-10ng/uL range.

Library preparation and sequencing were performed using the NEB Ultra II FS DNA PCR-free Library Prep Kit following the standard protocol on a Hamilton Liquid Handling Robot except for modifications: SPRI cleanup following ligation was performed with a single sided cleanup step, following library preparation 10 cycles of PCR were performed to amplify reads. Libraries were pooled at 120pM in 1,000uL and sequencing was performed on an UltimaGenomics sequencer with the Baseline 1.5 workflow, performing 116 cycles for 300bp length read sequencing.

Sequence files were trimmed and cleaned by trim_galore[59]. Sequences matched to the downloaded human genome GRCh38 through bowtie2 (2.5.2) were removed. Incomplete or small files and files with low median sequence length (<100bp) were removed. Duplication level, GC distribution, length distribution, and QC value were also checked. Taxonomy level quantification was performed by ChocoPhlAn and functional unit level quantification and normalization was performed by HUMAnN3 (3.0.1) with mpa_v30_CHOCOPhlAn_201901 index[60]. We quantified gene families, reactions, Gene Ontology (GO), KEGG, and pathways. Default parameters were used if not specified.

We used relative quantification for functional units and absolute quantification for taxonomy units. We used *Imtechella halotolerans* as the spike-in reference strain and sample weight to calculate

the absolute quantification. Samples with no measured reads from the reference strain or sample weight were removed. Features were filtered if they were labeled as unmapped, unintegrated, ungrouped, or unclassified. Taxonomy-specific functional features were removed if they were missing in more than 90% of samples.

Diversity was calculated with scikit-bio[61]. For alpha diversity, we calculated Chao1 richness, Gini index, the number of distinct operational taxonomic units (OTUs), Shannon entropy, and Simpson's index. For beta diversity, we calculated Jaccard distances and Bray-Curtis distances.

Omics integration

Metabolomics and lipidomics data were normalized by probabilistic quotient normalization (PQN) [62]. For metabolomics, only levels 1 and 2 with annotated names were kept for downstream analysis. Multiple batches in metabolomics and lipidomics were merged by scaling through the median in each batch. Metabolomics, lipidomics, and microbiome data were log-transformed to obtain better statistical distribution, while proteomics was already in the log scale. For association analysis, values from multiple samples of different visits of the same individuals were merged by average.

Pathway enrichment

We applied over-representative tests for metabolomics, lipidomics, and proteomics for significant features from statistical tests. In metabolomics and lipidomics, the enrichment was based on HMDB and KEGG IDs. For lipidomics, programs from Rodin and Lipid Mini-On were also used[63]. For proteomics, we used UniProt, Entrez, and Ensembl IDs for GO, KEGG, and Reactome enrichment. Only Cardiometabolic panels from Olink were kept as relevant features for enrichment. Used R packages included clusterProfiler, org.Hs.eg.db, ReactomePA, metpath, and KEGG.db for enrichment[64].

Statistical analysis

We used Spearman correlation calculated by 'cor' and 'cor.test'. When correcting for numerical covariates was needed, partial Spearman correlation by 'pcor.test' in the ppcor package was used[65]. The linear model was also used to correct for multiple covariates and validate results from Spearman correlation and group-wise tests. The association of numerical values was based on all available data if not otherwise specified. Categorical variables with two classes were represented as -0.5 and 0.5 in the linear model. T-tests (two-sided) were used to compare groups with effect size calculated by Cohen's d. Principal component analysis (PCA) and principal coordinates analysis (PCoA) were used for plotting and projection. In the boxplot, the default test and p-value adjustment (Mann-Whitney test, two-sided, Holm) between the two groups were used. Otherwise, FDR was used for multiple test corrections. Most statistical analysis was performed using R (version 4.2.1). The detailed version of all the packages is available in the Supplementary Note.

Mediation analysis

We used mediation analysis (R package mediation) to study the effects of microbiome mediated through metabolomics and lipidomics on outcomes (clinical measurements and PPGRs to

carbohydrate meals) [36,37]. To reduce the number of possible edges between omics, we filter by only selecting strong feature pairs in prior analysis. The tables of possible features to test were filtered by the Spearman correlation test from the microbiome to outcomes (FDR<0.1) and from the microbiome to mediators (FDR<0.05). Covariates include sex, BMI, and the weights of microbiome samples. A reverse analysis was implemented to remove false positives[36]. Default parameters were used if not otherwise specified. In the reverse analysis, we exchanged the roles of mediators and outcomes. Any results that were also significant in the reverse analysis were removed.

Regression models

We developed machine learning regression models to evaluate the predictive value of omics data on SSPG and to identify strong predictive features. CGM data were grouped by participant and meal type, with mean values computed for each group. We used omics data from the Omics integration section (Methods Section 14).

To build the models, the data was split into a training (95% of data) and a test set. Each sample was one participant, and we had 38 participants for the model building. Our dataset was composed of 3 feature sets, namely clinical (including fasting insulin, fasting glucose, HbA1c, BMI, age, and sex), metabolites (731 features), and lipids (654 features). Each feature set from the training set was used to build separate ElasticNet regression models to identify relevant predictors, with cross-validation used to select the optimal regularization parameters to minimize mean squared error (MSE) [66]. ElasticNet was chosen because of our relatively small sample size.

We used multiple approaches to efficiently merge information from different feature sets (fusion) and further improve performance. We explored two fusion strategies, early and late fusion. Early fusion combined all feature sets into a single model using ElasticNet regression, while late fusion first trained ElasticNet models individually on each feature set and then combined their predictions using linear regression. Furthermore, we used cooperative learning that encompasses both early and late fusion and leverages interdependencies among feature sets[67]. This method jointly optimized coefficients across multiple views and encourages agreement between the views. The agreement penalty parameter was selected through cross validation.

Each of these models was built 100 times with different train/test splits. Results were then averaged across all the repetitions. We reported the strongest features from the cooperative learning model by ranking the average of the absolute value of the coefficients across all simulations. We also built models to estimate the ratio between potato and grape peaks and most settings were kept the same except that SSPG was added in clinical features for this prediction.

Starch analysis

Four standardized carbohydrate meals were prepared in the same way as for participants. The starch composition was measured according to published methods and biochemical assay (K-DSTRS) [68]. Rapidly digestible starch (RDS) is the starch that is digested within 20 minutes, slowly digestible starch (SDS) is the starch that is digested between 20 minutes and 120 minutes, and

resistant starch is the starch that's not digested within 4 hours. The foods were rapidly frozen by liquid nitrogen and grinded before the assay.

Reference:

56. Contrepois, K., Jiang, L. & Snyder, M. Optimized Analytical Procedures for the Untargeted Metabolomic Profiling of Human Urine and Plasma by Combining Hydrophilic Interaction (HILIC) and Reverse-Phase Liquid Chromatography (RPLC)–Mass Spectrometry *^[S]. *Molecular & Cellular Proteomics* **2015**, 14 (6), 1684-1695. DOI: 10.1074/mcp.M114.046508 (acccessed 2024/05/24).
57. Fan, S., Kind, T., Cajka, T., Hazen, S. L., Tang, W. H. W., Kaddurah-Daouk, R., Irvin, M. R., Arnett, D. K., Barupal, D. K. & Fiehn, O. Systematic Error Removal Using Random Forest for Normalizing Large-Scale Untargeted Lipidomics Data. *Analytical chemistry* **2019**, 91 (5), 3590-3596. DOI: 10.1021/acs.analchem.8b05592.
58. Contrepois, K., Mahmoudi, S., Ubhi, B. K., Papsdorf, K., Hornburg, D., Brunet, A. & Snyder, M. Cross-Platform Comparison of Untargeted and Targeted Lipidomics Approaches on Aging Mouse Plasma. *Sci Rep* **2018**, 8 (1), 17747. DOI: 10.1038/s41598-018-35807-4 From NLM Medline.
59. Martin, M. Cutadapt removes adapter sequences from high-throughput sequencing reads. *EMBnet.journal; Vol 17, No 1: Next Generation Sequencing Data AnalysisDO - 10.14806/ej.17.1.200* **2011**.
60. Beghini, F., McIver, L. J., Blanco-Miguez, A., Dubois, L., Asnicar, F., Maharjan, S., Mailyan, A., Manghi, P., Scholz, M., Thomas, A. M. *et al.* Integrating taxonomic, functional, and strain-level profiling of diverse microbial communities with bioBakery 3. *Elife* **2021**, 10. DOI: 10.7554/eLife.65088 From NLM Medline.
61. Yu, H., Li, M., Sandhu, J., Sun, G., Schnable, J. C., Walia, H., Xie, W., Yu, B., Mower, J. P. & Zhang, C. Pervasive misannotation of microexons that are evolutionarily conserved and crucial for gene function in plants. *Nature Communications* **2022**, 13 (1), 820. DOI: 10.1038/s41467-022-28449-8.
62. Dieterle, F., Ross, A., Schlotterbeck, G. & Senn, H. Probabilistic Quotient Normalization as Robust Method to Account for Dilution of Complex Biological Mixtures. Application in 1H NMR Metabonomics. *Analytical chemistry* **2006**, 78 (13), 4281-4290. DOI: 10.1021/ac051632c.
63. Clair, G., Reehl, S., Stratton, K. G., Monroe, M. E., Tfaily, M. M., Ansong, C. & Kyle, J. E. Lipid Mini-On: mining and ontology tool for enrichment analysis of lipidomic data. *Bioinformatics* **2019**, 35 (21), 4507-4508. DOI: 10.1093/bioinformatics/btz250 (acccessed 5/24/2024).
64. Wu, T., Hu, E., Xu, S., Chen, M., Guo, P., Dai, Z., Feng, T., Zhou, L., Tang, W., Zhan, L. *et al.* clusterProfiler 4.0: A universal enrichment tool for interpreting omics data. *Innovation (Camb)* **2021**, 2 (3), 100141. DOI: 10.1016/j.xinn.2021.100141 From NLM PubMed-not-MEDLINE.
65. Kim, S. ppcor: An R Package for a Fast Calculation to Semi-partial Correlation Coefficients. *Commun Stat Appl Methods* **2015**, 22 (6), 665-674. DOI: 10.5351/CSAM.2015.22.6.665 From NLM PubMed-not-MEDLINE.
66. Zou, H. & Hastie, T. Regularization and Variable Selection Via the Elastic Net. *Journal of the Royal Statistical Society Series B: Statistical Methodology* **2005**, 67 (2), 301-320. DOI: 10.1111/j.1467-9868.2005.00503.x (acccessed 7/1/2024).

67. Ding, D. Y., Li, S., Narasimhan, B. & Tibshirani, R. Cooperative learning for multiview analysis. *Proceedings of the National Academy of Sciences of the United States of America* **2022**, 119 (38), e2202113119. DOI: 10.1073/pnas.2202113119 From NLM Medline.
68. Englyst, H. N., Kingman, S. M. & Cummings, J. H. Classification and measurement of nutritionally important starch fractions. *Eur J Clin Nutr* **1992**, 46 Suppl 2, S33-50. From NLM Medline.

Supplementary Figures

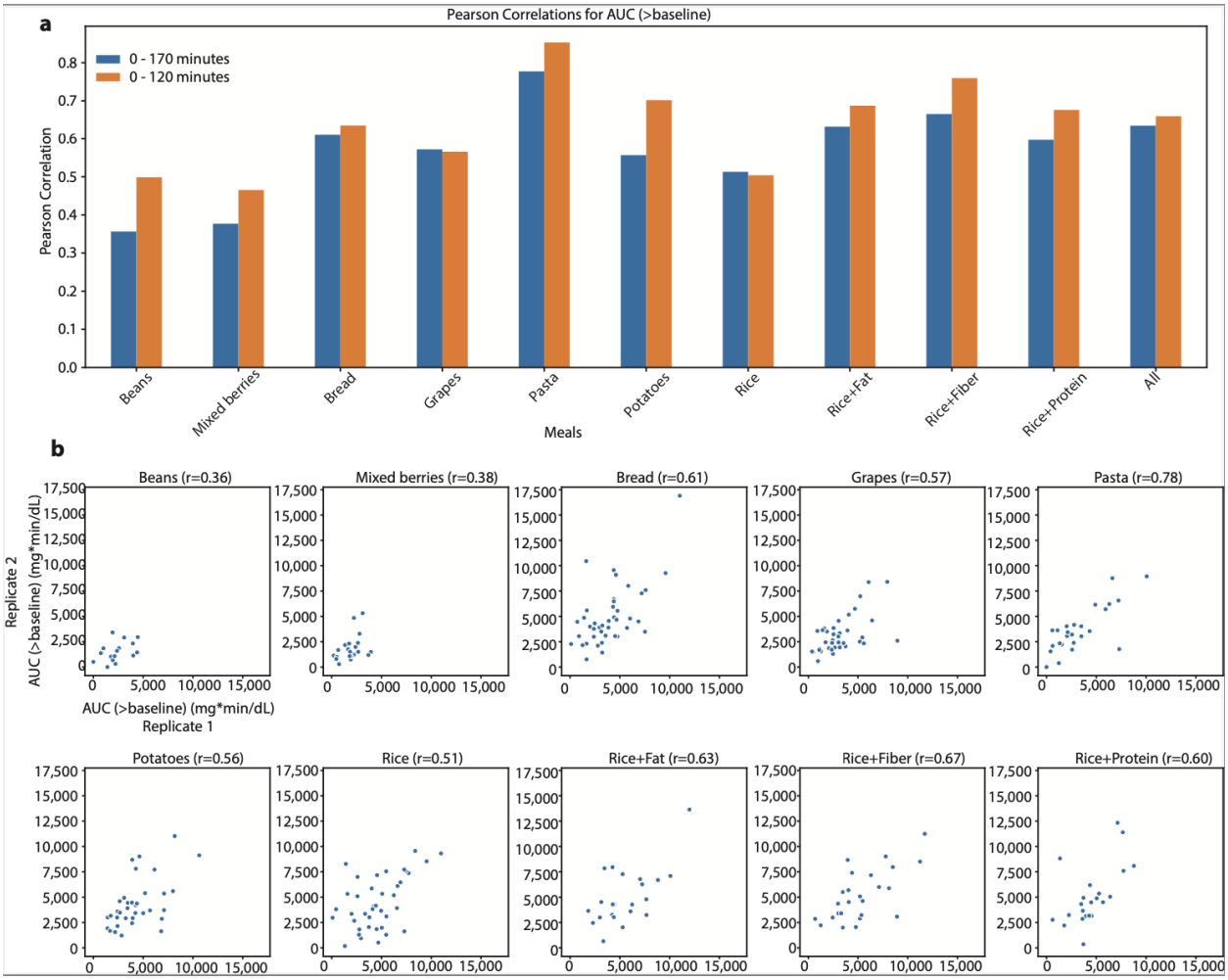

Figure S1: Consistency of CGM curves between replicates. a: Pearson correlation between AUC(>baseline) of two available replicates for each standardized meal. All indicates all standardized carbohydrate meals without mitigator foods were used in the computation. Correlation of AUC(>baseline) was calculated for both 170 minutes postprandial (blue) and 120 minutes (orange) data. **b**: Scatter plot of AUC(>baseline) for 170 minutes.

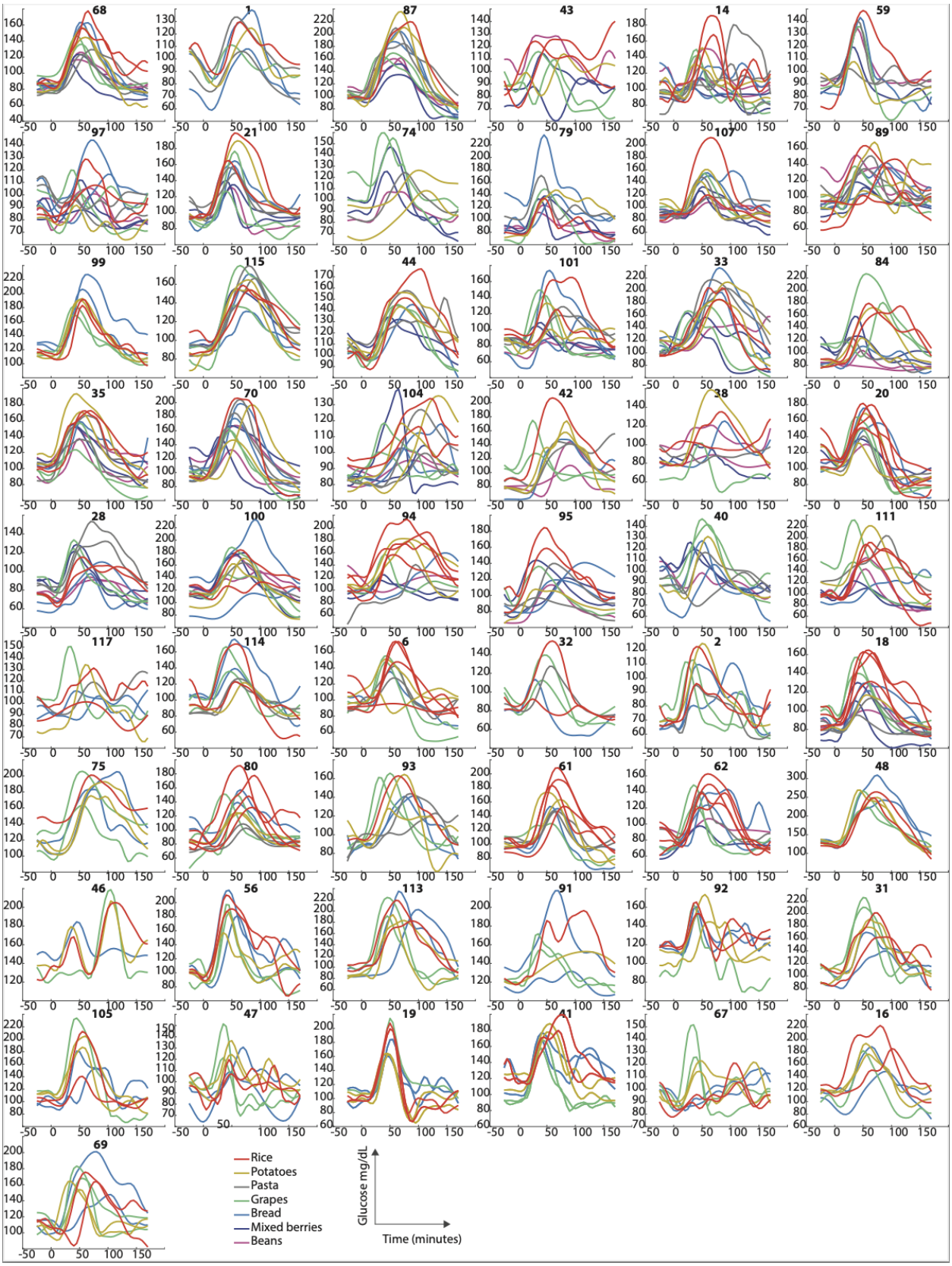
Rice
Potatoes
Pasta
Grapes
Bread
Mixed berries
Beans
Glucose mg/dL
Time (minutes)

Figure S2: CGM curves of all standardized carbohydrate meals. CGM curves of 55 participants are presented with the X-axis for time (minute) and the Y-axis for glucose level (mg/dL). Different carbohydrate meals are visualized by different colors and all replicates are presented. Each figure shows the CGM-measured PPGRs of one participant with the participant id as the title.

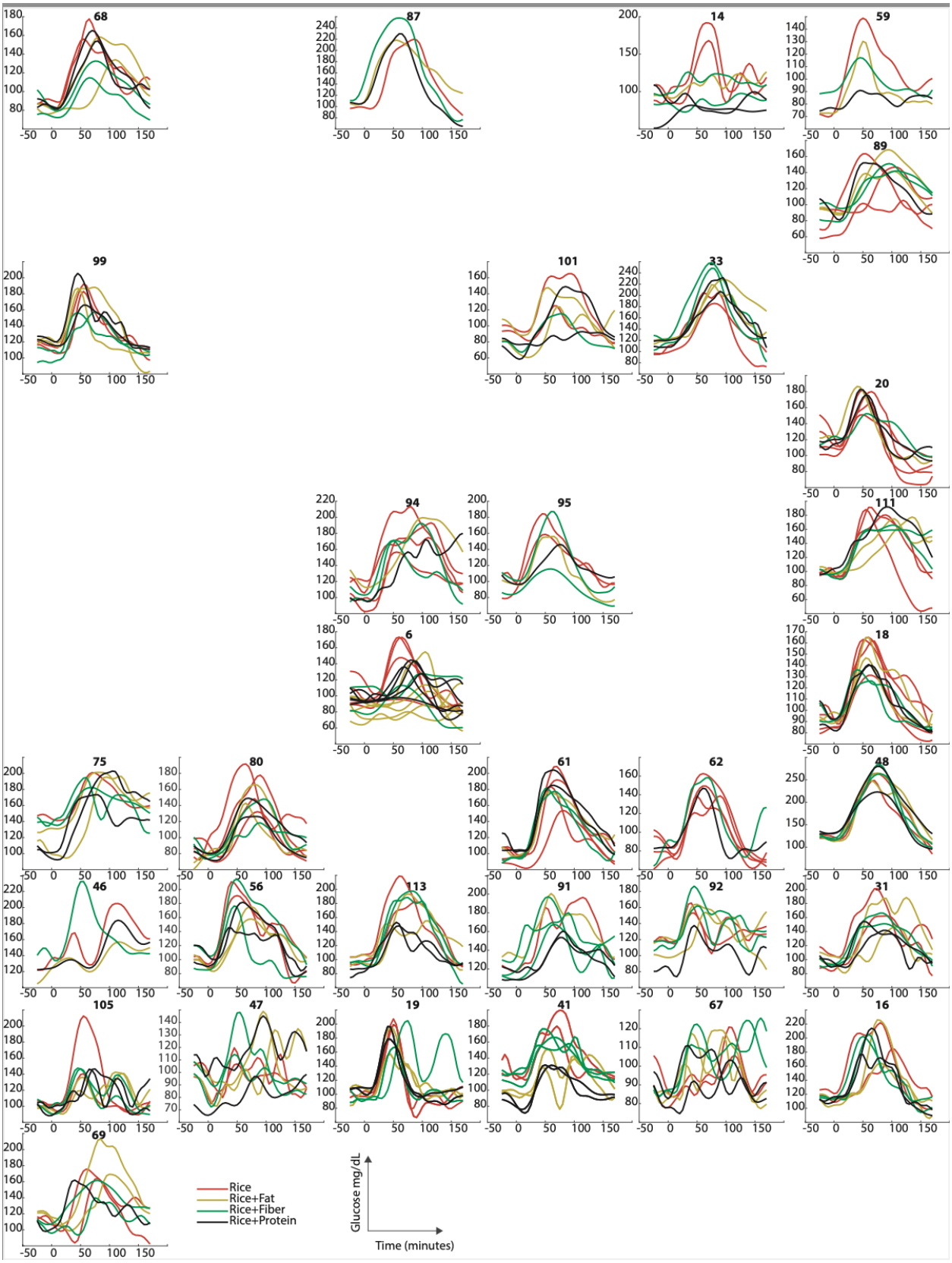
68
87
14
59
89
99
101
33
20
94
95
111
6
18
75
80
61
62
48
46
56
113
91
92
31
105
47
19
41
67
16
69
Rice
Rice+Fat
Rice+Fiber
Rice+Protein
Glucose mg/dL
Time (minutes)

Figure S3: CGM curves of all rice and rice + mitigators. CGM curves of 55 participants are presented with the X-axis for time (minute) and the Y-axis for glucose level (mg/dL). The figure is formatted and ordered the same way as Fig. S2 with empty space indicating a lack of good CGM data on mitigator foods for the individual. Different food combinations are visualized by different colors and all replicates are presented. Each figure shows the CGM-measured PPGR of one participant with the participant id as the title.

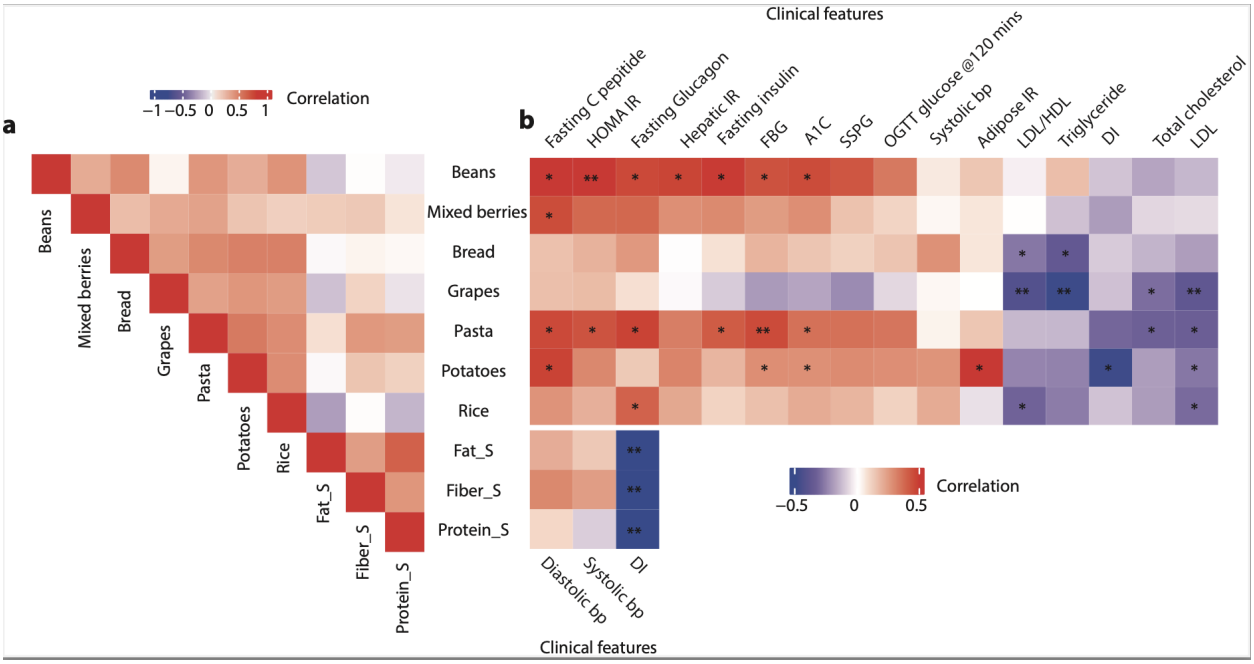

Figure S4: Expanded view of the association between metabolic traits and PPGRs of different carbohydrate meals and mitigation effects. a is the same as Figure 2A and is presented here for easy co-visualization together with b. **b**: Spearman correlation between PPGRs (standardized meal delta glucose peak and mitigator effect) and clinical measurements. Red indicates positive and blue indicates negative correlation. Asterisks indicate p-value <0.05 and double asterisks indicate pFDR<0.1. FDR corrections were implemented for the whole correlation matrix. Features are clustered. A similar plot of AUC (>baseline) can be found in Fig. S7.

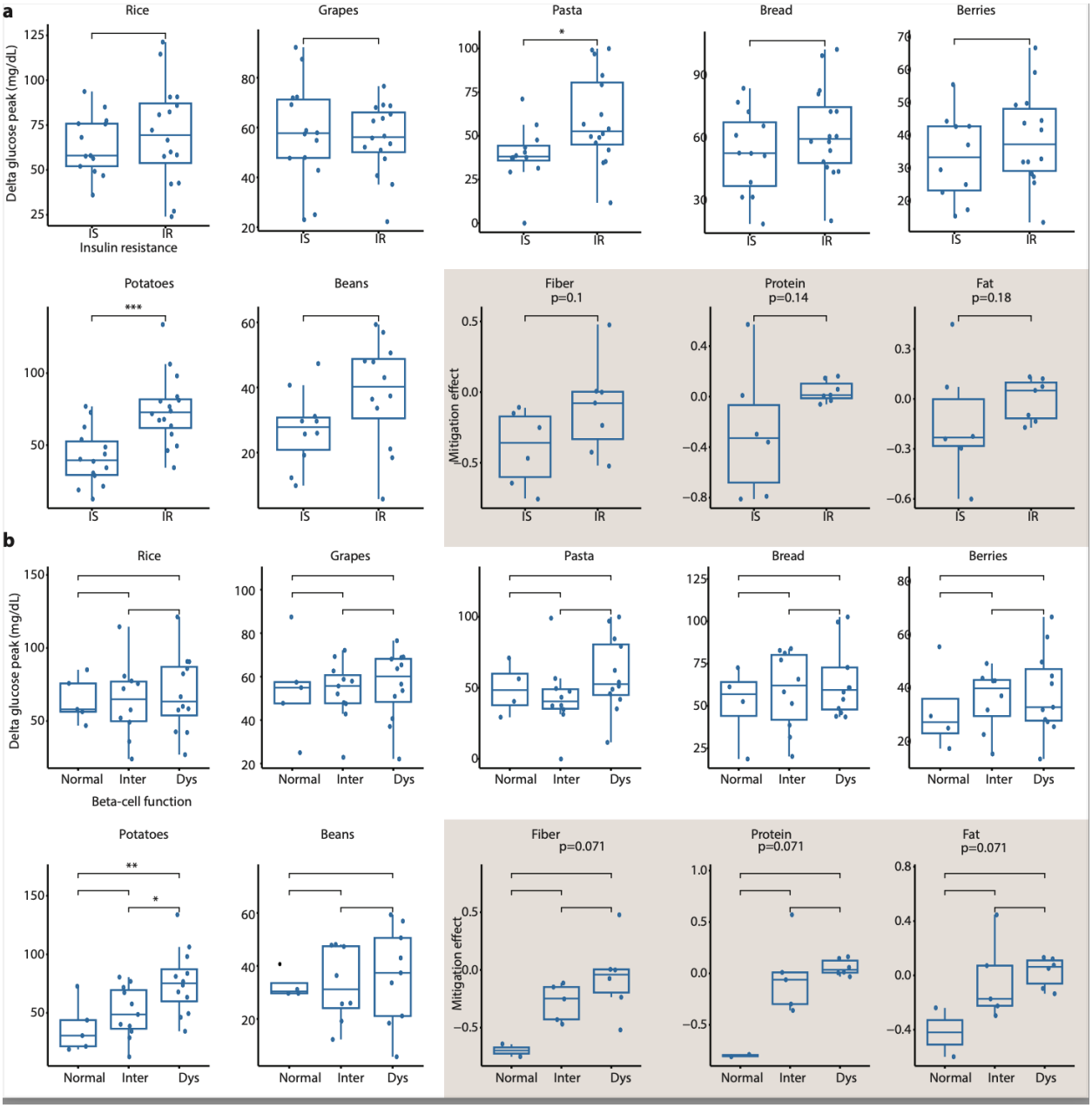

Figure S5: Comparison of postprandial glycemic peaks between individuals with different levels of insulin resistance and beta cell function. a: Delta glucose peak (mg/dL) and mitigation effect (based on delta glucose) between individuals who are insulin resistant (IR) and insulin sensitive (IS) measured by SSPG. Each figure is for one different meal, and the boxplot shows the delta glucose peak for standardized carbohydrate meals and the mitigation effect for mitigator foods (gray shades). *: based on Holm corrected p-value of the Mann-Whitney test (two-sided, default) of selected pairs, *: p_H<=0.05, **: p_H<=0.01, ***: p_H<=0.001. The exact p_H are listed in figure 3. **b**: Delta glucose peak and mitigation effect (based on delta glucose) between individuals with normal, dysfunctional, and intermediate beta cell function. Beta cell function is quantified using DI which is adjusted by SSPG. The number of participants for IS (IR) in a is rice

13 (16), grapes 14 (16), pasta 12 (16), bread 12 (16), berries 10 (14), potatoes 14 (16), beans 10 (12), fiber 6 (7), protein 6 (7), and fat 6 (7). The number of participants for normal (intermediate, dysfunctional) beta cell function in b is rice 5 (10, 12), grapes 5 (11, 12), pasta 4 (10, 12), bread 4 (10, 12), berries 4 (8, 11), potatoes 5 (11, 12), beans 4 (8, 9), fiber 2 (5, 6), protein 2 (5, 6), and fat 2 (5, 6). Extracted CGM features for each participant are compared between different metabolic subtypes. The boxplots show the center line as the median and the hinges as the 25th and 75th percentiles. The upper whisker extends from the hinge to the largest value not bigger than 1.5 times the distance between the hinges. Data beyond the whiskers are outliers.

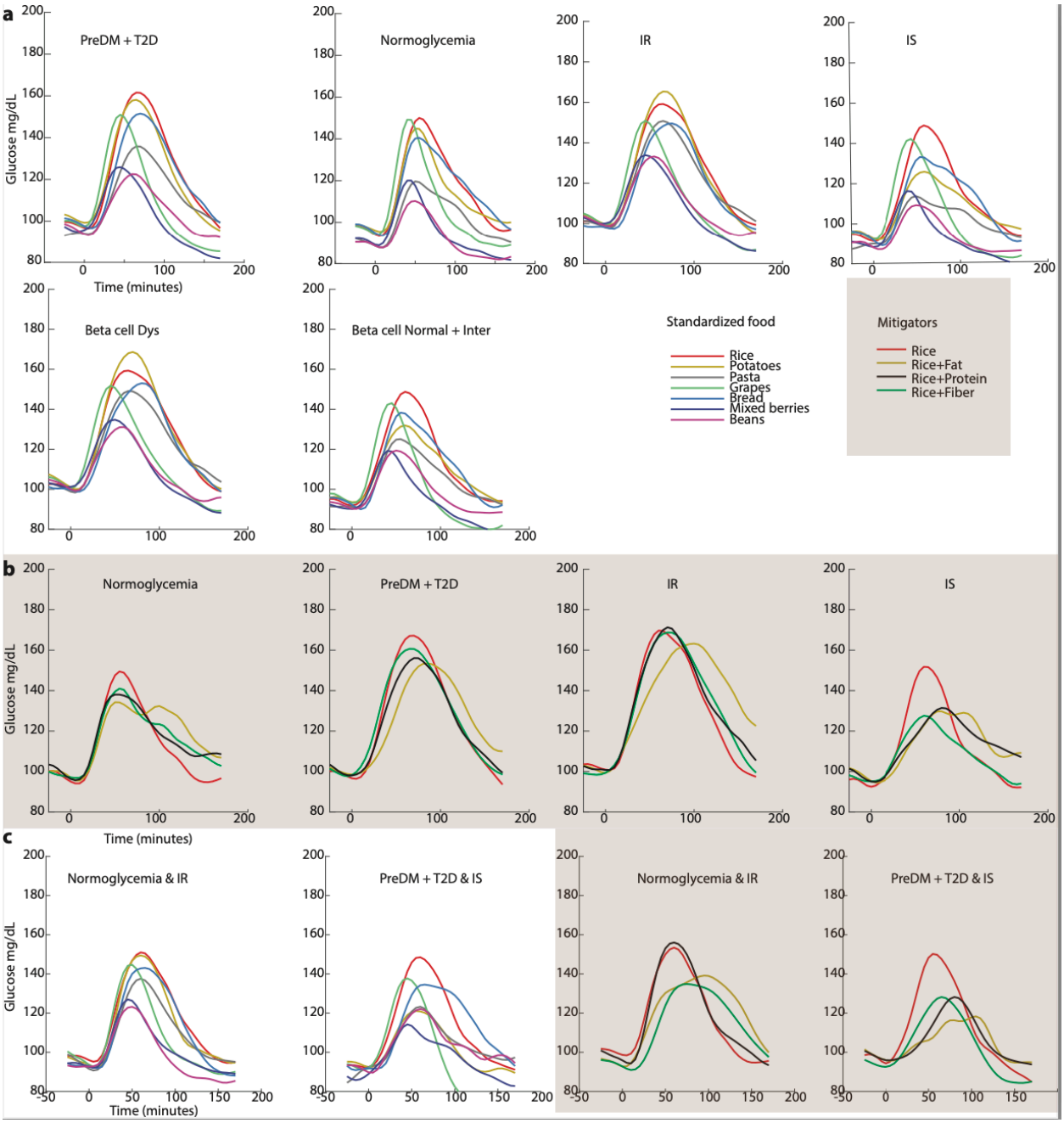

Figure S6: mean postprandial CGM curves between different metabolic function subgroups. **a**: the average of standardized meal curves between groups separated by different clinical features regarding metabolic function, including T2D status (normoglycemia vs PreDM and T2D), insulin resistance measured by SSPG (IS vs IR), and beta cell functions (dysfunction vs intermediate and normal). Curves showing mitigator effects are highlighted in gray shades. **b**: rice + mitigator curves between groups separated by different clinical features, including T2D status and insulin resistance measured by SSPG. In participants with mitigator data in our cohort, the group with dysfunctional (normal, intermediate) beta cells largely overlaps with the IR (IS) group. **c**: curves of standardized carbohydrate meals and mitigator foods for the intersection group, including normoglycemia with IR and PreDM or T2D with IS. The X-axis is time (minute),

and the Y-axis is glucose level (mg/dL). Metabolic traits based stratification is based on group 1 (Details in Methods). Abbreviations: PreDM: prediabetes; T2D: type 2 diabetes; IR: insulin resistance; IS: insulin sensitive; Dys: beta cell dysfunction; inter: beta cell intermediate function.

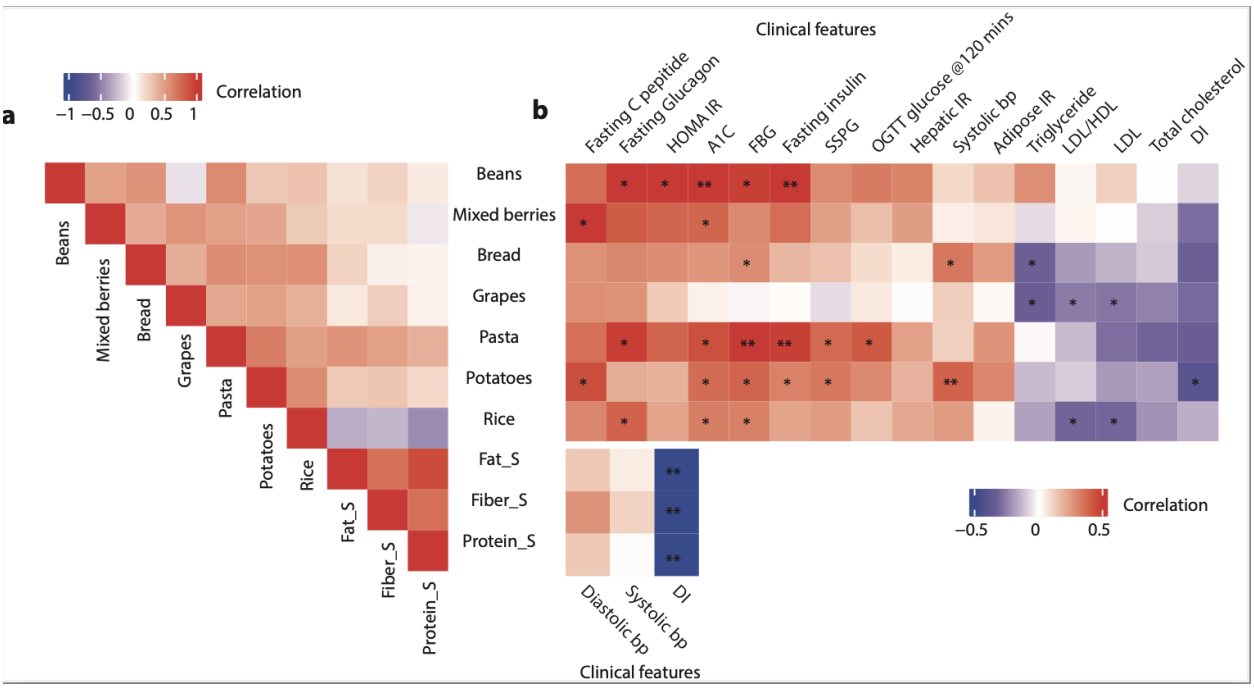

Figure S7: Expanded view of the association between metabolic traits and PPGRs of different meals and mitigation effects based on AUC (>baseline). a: the Spearman correlation between PPGRs of all different meals, including both AUC (>baseline) of standardized carbohydrate meals and the suppression effect of mitigator foods. The suppression mitigator effects here were defined by subtracting the AUC (>baseline) of rice + mitigator from that of rice and then normalizing it by that of rice. **b**: Spearman correlation between PPGRs (standardized meal AUC (>baseline) and mitigator effect) and clinical measurements. Red indicates positive, and blue indicates negative correlation. Asterisks indicate p-value <0.05 and double asterisks indicate pFDR<0.1. FDR corrections were implemented for the whole correlation matrix. Features are clustered. A similar plot of delta glucose peak changes can be found in Fig. S4.

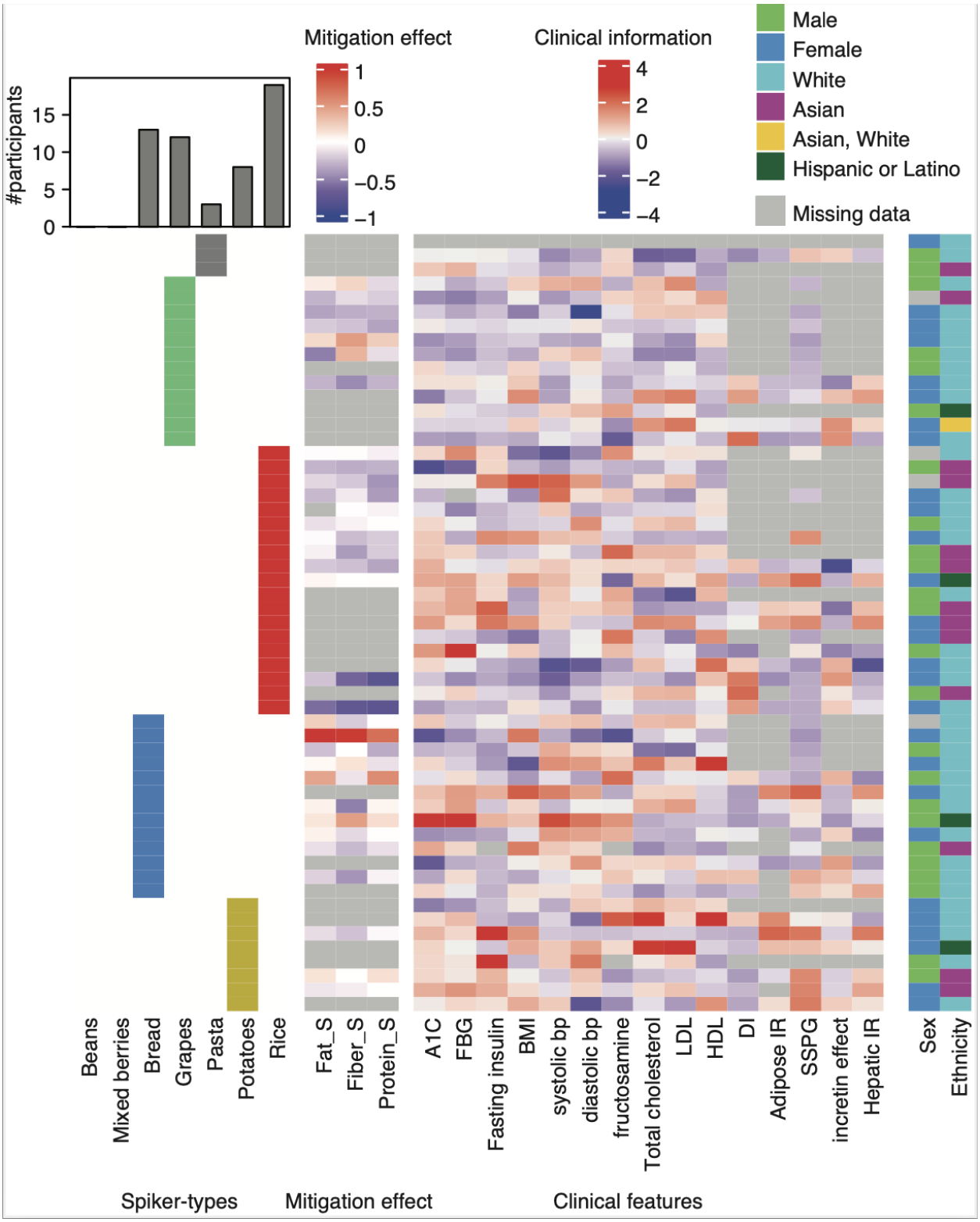

Figure S8: Heatmap of carb-response-types, mitigation effect, and selected clinical and demographic information. Each row is a participant, and the left panel shows carb-response-types, judged by the carbohydrate meals with the highest PPGR for the individual measured by delta glucose peak. The heatmap is clustered by carb-response-types. The second from the left

panel shows relative mitigation effects with red increasing effects and blue decreasing effects. The third one shows levels of different numerical values in clinical measurements with red high and blue low. The remaining parts show some categorical metadata as labeled in the legends. The grey color indicates missing data. The top left bar plot shows the number of participants for each carb-response-type.

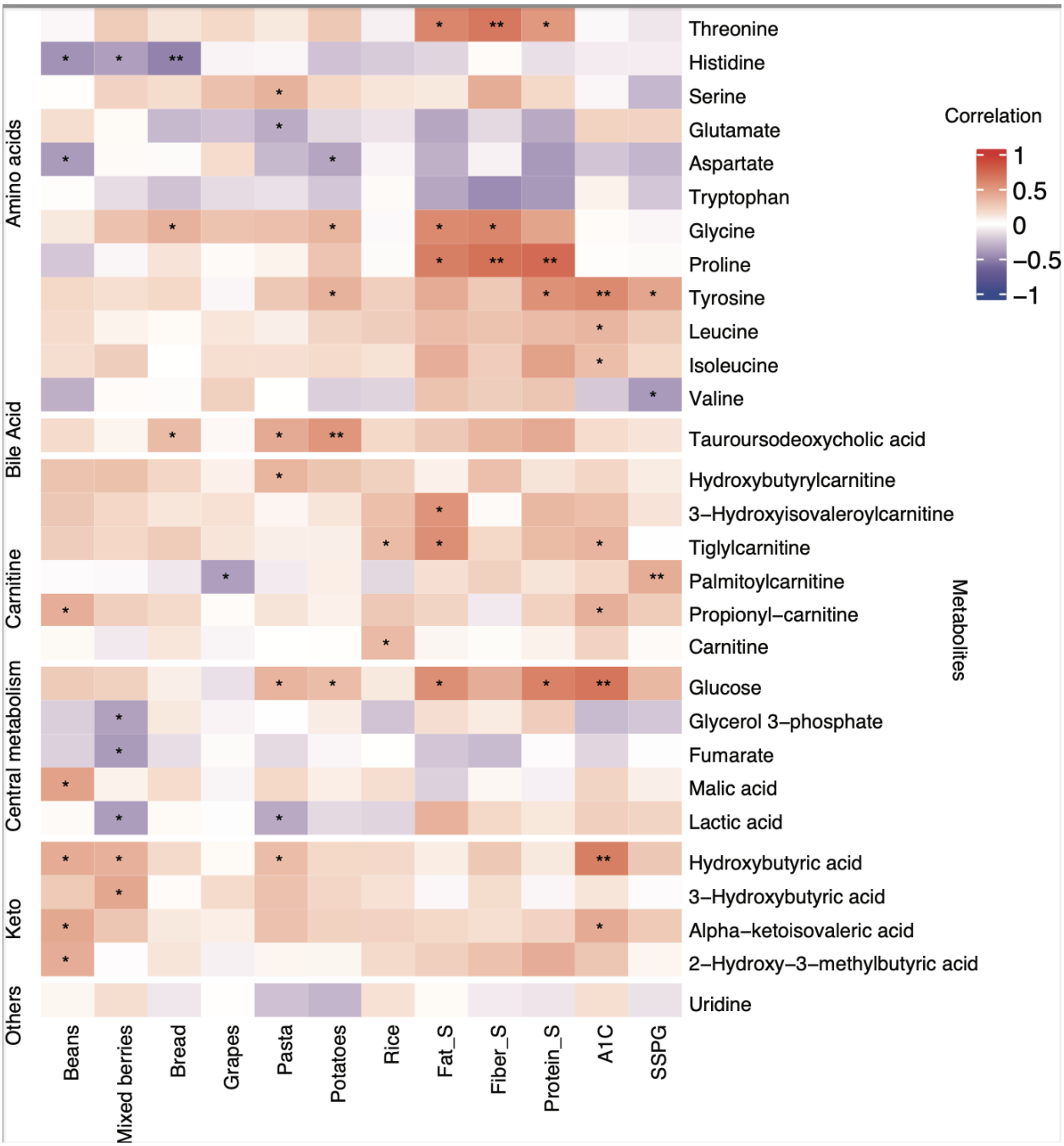

Figure S9: Spearman correlation between PPGRs and metabolomics. Common metabolic features are presented in rows and grouped by functional pathways. PPGRs to carbohydrate meal, mitigation effect, and two clinical features are presented in columns. A1C and SSPG are included to check known associations. Red indicates positive, and blue indicates negative correlation. Asterisks indicate p-value <0.05 and double asterisks indicate pFDR<0.2. FDR corrections were implemented for the whole correlation matrix.

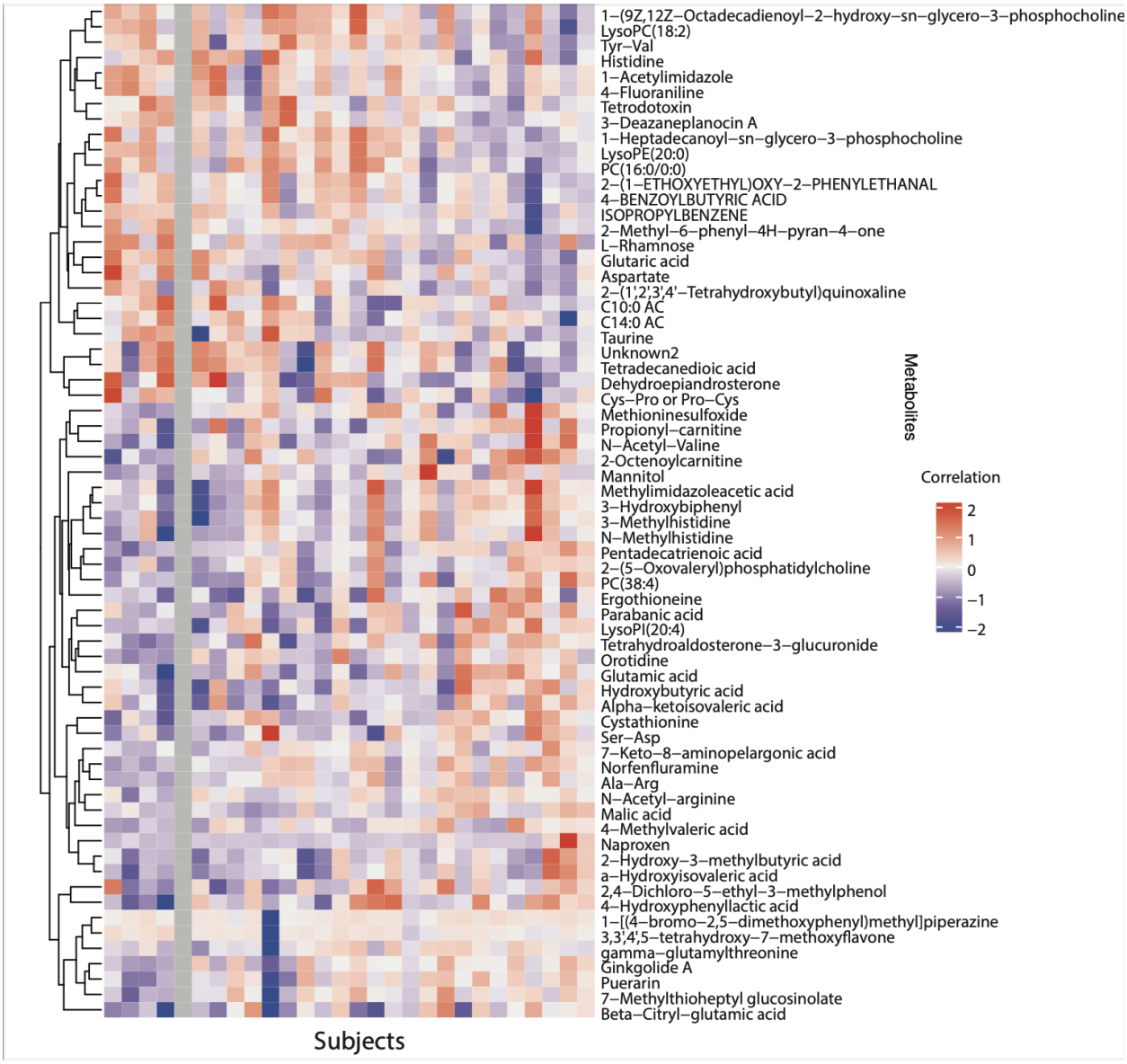

Figure S10: Heatmap of bean spike associated metabolites. Each row is one metabolite that's correlated (Spearman) with PPGRs to beans (p-value <0.05). Each column is one participant. The participants are ordered so that the left side has lower bean spikes, and the right side has higher bean spikes. The grey color is missing value, red indicates higher, and blue indicates lower. Rows are clustered into metabolites that are positively or negatively correlated with bean spikes.

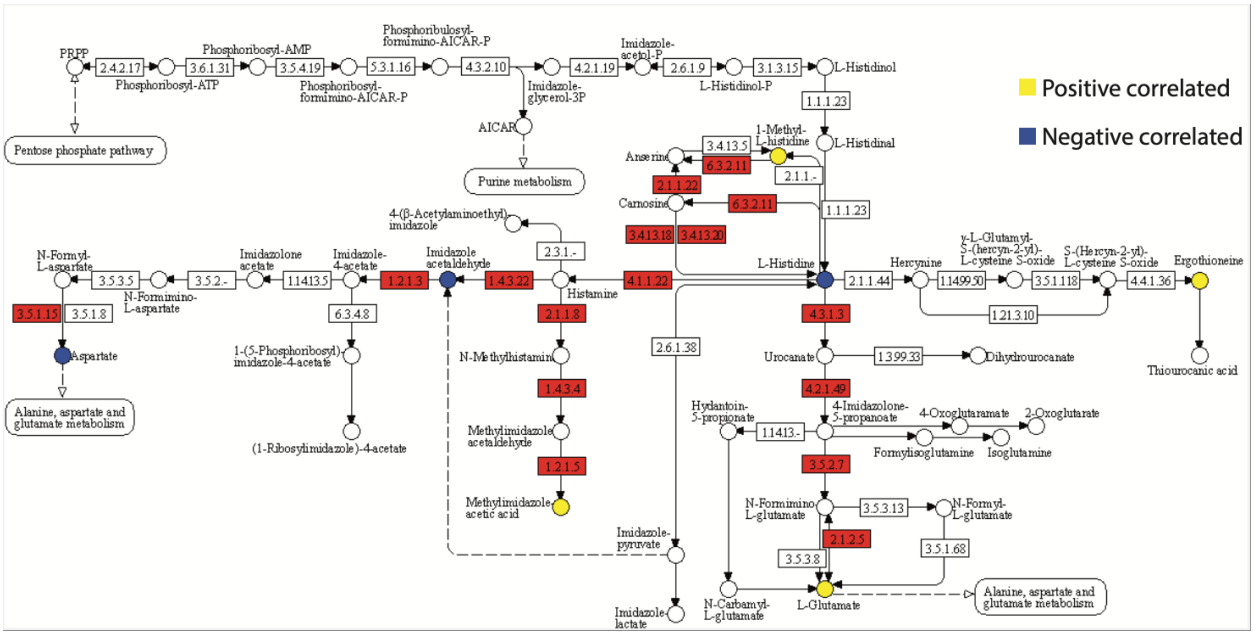

Figure S11: Histidine pathway visualized with metabolites associated with bean spikes. Small circles are metabolites, and rectangles are proteins (enzymes). Yellow (blue) indicates positive (negative) correlations with bean spikes (p-value<0.05). Proteins that exist in the human KEGG pathway are red.

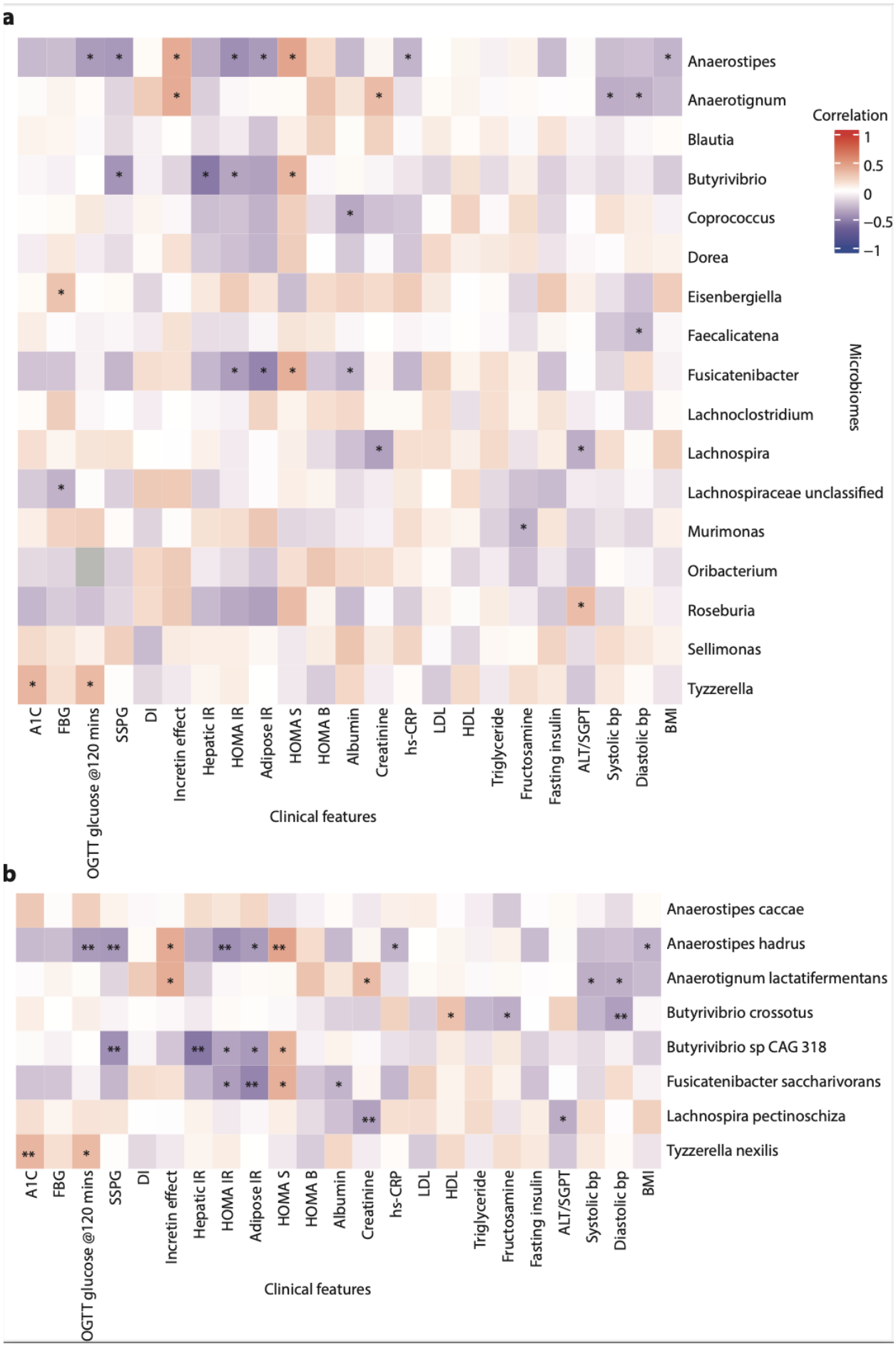
a
Anaerostipes
Anaerotignum
Blautia
Butyrivibrio
Coprococcus
Dorea
Eisenbergiella
Faecalicatena
Fusicatenibacter
Lachnoclostridium
Lachnospira
Lachnospiraceae unclassified
Murimonas
Oribacterium
Roseburia
Sellimonas
Tyzzerella
Microbiomes
Correlation
1
0.5
0
−0.5
−1
A1C
FBG
OGTT glcuose @120 mins
SSPG
DI
Incretin effect
Hepatic IR
HOMA IR
Adipose IR
HOMA S
HOMA B
Albumin
Creatinine
hs-CRP
LDL
HDL
Triglyceride
Fructosamine
Fasting insulin
ALT/SGPT
Systolic bp
Diastolic bp
BMI
Clinical features
b
Anaerostipes caccae
Anaerostipes hadrus
Anaerotignum lactatifermentans
Butyrivibrio crossotus
Butyrivibrio sp CAG 318
Fusicatenibacter saccharivorans
Lachnospira pectinoschiza
Tyzzerella nexilis
A1C
FBG
OGTT glucose @120 mins
SSPG
DI
Incretin effect
Hepatic IR
HOMA IR
Adipose IR
HOMA S
HOMA B
Albumin
Creatinine
hs-CRP
LDL
HDL
Triglyceride
Fructosamine
Fasting insulin
ALT/SGPT
Systolic bp
Diastolic bp
BMI
Clinical features

Figure S12: Spearman correlation between clinical measurements and the Lachnospiraceae family. a: Each genus in the Lachnospiraceae family is associated with clinical features. Red indicates positive, and blue indicates negative correlation. **b**: species in selected genera are associated with clinical features. Asterisks indicate p-value <0.05 and double asterisks indicate pFDR<0.3. FDR corrections were implemented for the whole correlation matrix.

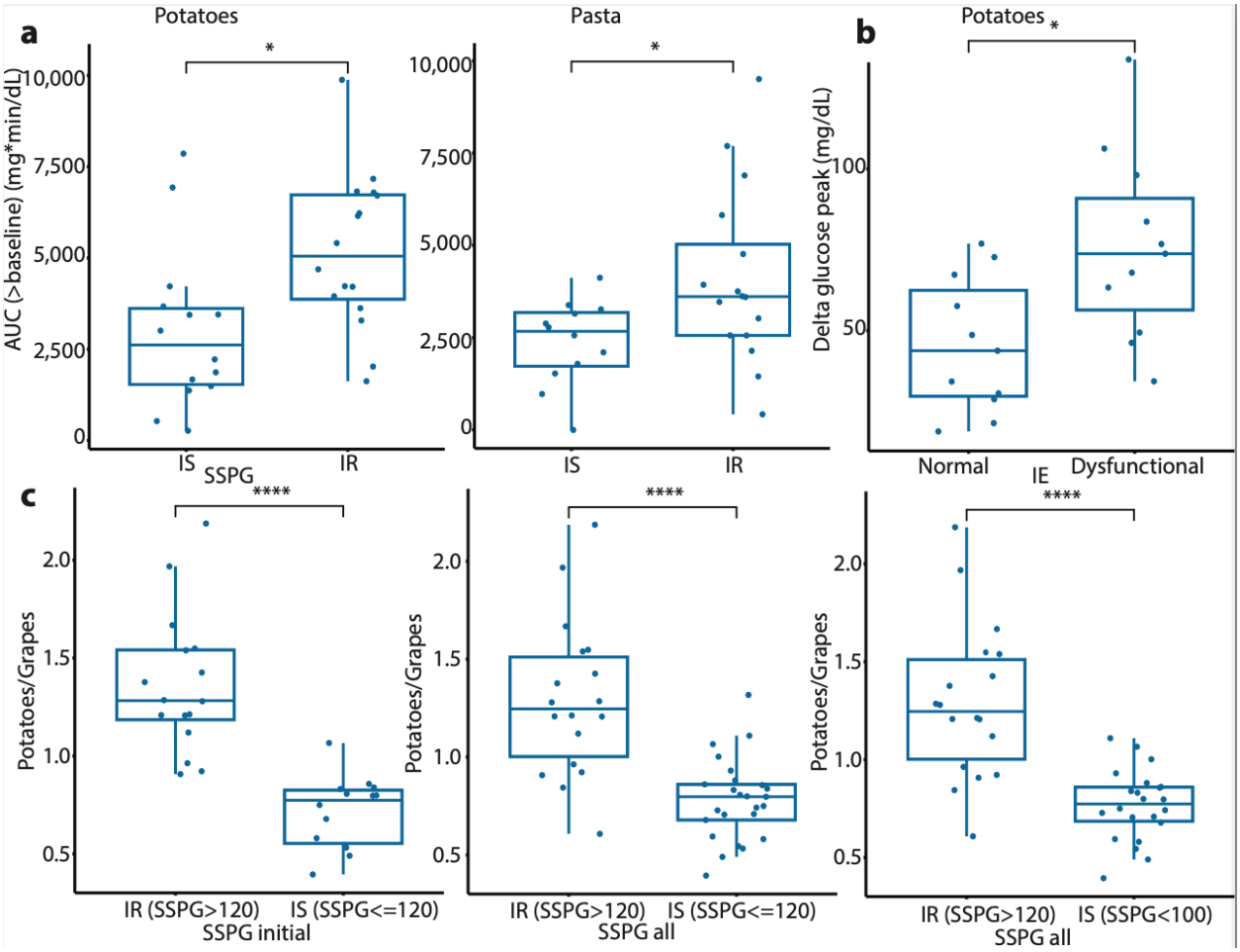

Figure S13: Additional support for glycemic response between metabolic trait subtypes. **a**: glycemic peaks between individuals who are insulin resistant (IR) and insulin sensitive (IS) measured by AUC (>baseline) (mg*min/dL). Each figure is for one different carbohydrate meal and the boxplot shows AUC (>baseline) for standardized carbohydrate meals. The two carbohydrate meals with strong results from Fig. S5 were selected *: based on Holm corrected p-value of the Mann-Whitney test (default) of selected pairs, *: p_H<=0.05. **b**: Comparison of glycemic peaks (mg/dL) between individuals with normal and dysfunctional incretin function. The incretin function was measured through an alternative definition: Normal: IE%>60; Dysfunctional: IE%<40%. The test was not significant with the default IE threshold. **c**: Comparison of the ratio between the delta glucose peak of potatoes and that of grapes between IR and IS. The comparison was done in both the initial cohort with relatively complete metabolic test results (left) and the combined cohort with additional new SSPG collections (middle and right). Two different stratification methods were applied. The number of participants for IS (IR) in a is pasta 12 (16) and potatoes 14 (16). The number of participants for normal (dysfunctional) incretin effect in b is 11 (11). The number of participants for IS (IR) in c is 14 (16), 25 (18), and 22 (18) from left to right. Extracted CGM features for each participant are compared between different metabolic subtypes. The boxplots show the center line as the median and the hinges as the 25th and 75th percentiles. The upper whisker extends from the hinge to the largest value not bigger than 1.5

times the distance between the hinges. Data beyond the whiskers are outliers. The p_H from left to right top to bottom is 0.01, 0.033, 0.01, 9.8E-8, 2.2E-6, and 1.4E-6.

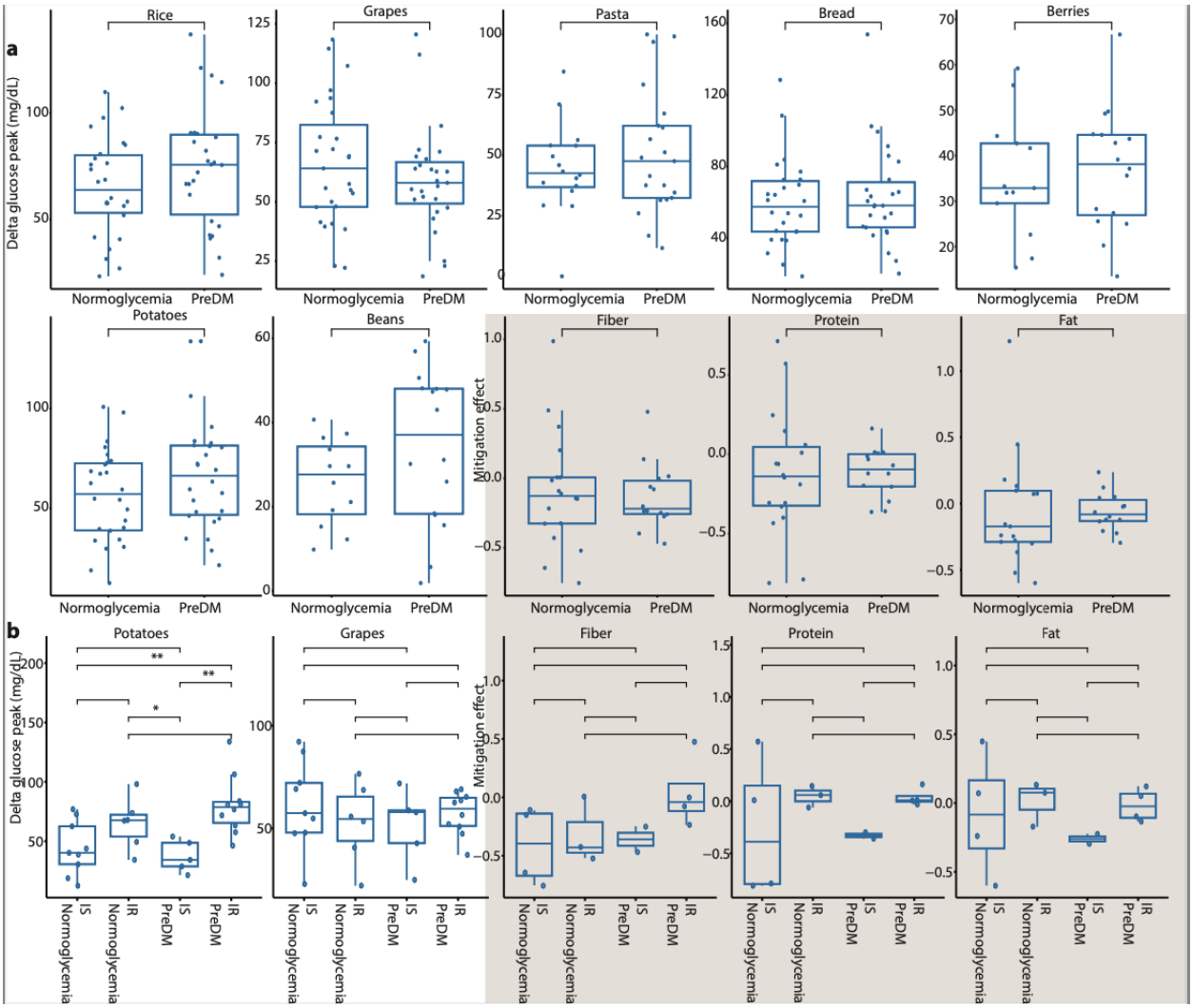

Figure S14: Different glycemic responses between participants with normoglycemia and PreDM and interaction with insulin resistance. a: Delta glucose peak (mg/dL) and mitigation effect (ratio) between individuals with normoglycemia and PreDM (including T2D) classified by HbA1c. Each figure is for one different meal and the boxplot shows the delta glucose peak for standardized carbohydrate meals and the mitigation effect for mitigator foods (gray shades). **b**: Delta glucose peak (mg/dL) and mitigation effect (ratio) between individuals of the four intersection groups of blood glucose and insulin resistance, including normoglycemia and insulin sensitive (IS), normoglycemia and insulin resistant (IR), PreDM (including T2D) and IS, and PreDM and IR. Normoglycemia and PreDM were classified by HbA1c. IS and IR were classified by SSPG. Each figure is for one different meal and the boxplot shows the delta glucose peak for standardized carbohydrate meals and the mitigation effect for mitigator foods (gray shades). *: based on Holm corrected p-value of the Mann-Whitney test (two-sided, default) of selected pairs, *: p_H<=0.05, **: p_H<=0.01. The number of participants for normoglycemia (PreDM) in a is rice 26 (26), grapes 27 (27), pasta 16 (21), bread 26 (26), berries 13 (16), potatoes 26 (26), beans 12 (16), fiber 18 (14), protein 18 (14), and fat 17 (14). The number of participants for normoglycemia IS (normoglycemia IR, PreDM IS, PreDM IR) in b is potatoes 9 (6, 5, 10), grapes 9 (6, 5, 10), fiber 4 (3, 2, 4), protein 4 (3, 2, 4), and fat 4 (3, 2, 4). Extracted CGM features for each participant are

compared between different metabolic subtypes. The boxplots show the center line as the median and the hinges as the 25th and 75th percentiles. The upper whisker extends from the hinge to the largest value not bigger than 1.5 times the distance between the hinges. Data beyond the whiskers are outliers. The p_H is: IR PreDM vs IS normoglycemia (left 1) 4.1E-3, IR PreDM vs IS PreDM (left 1) 2.7E-3, and IS PreDM vs IR normoglycemia (left 1) 0.03.

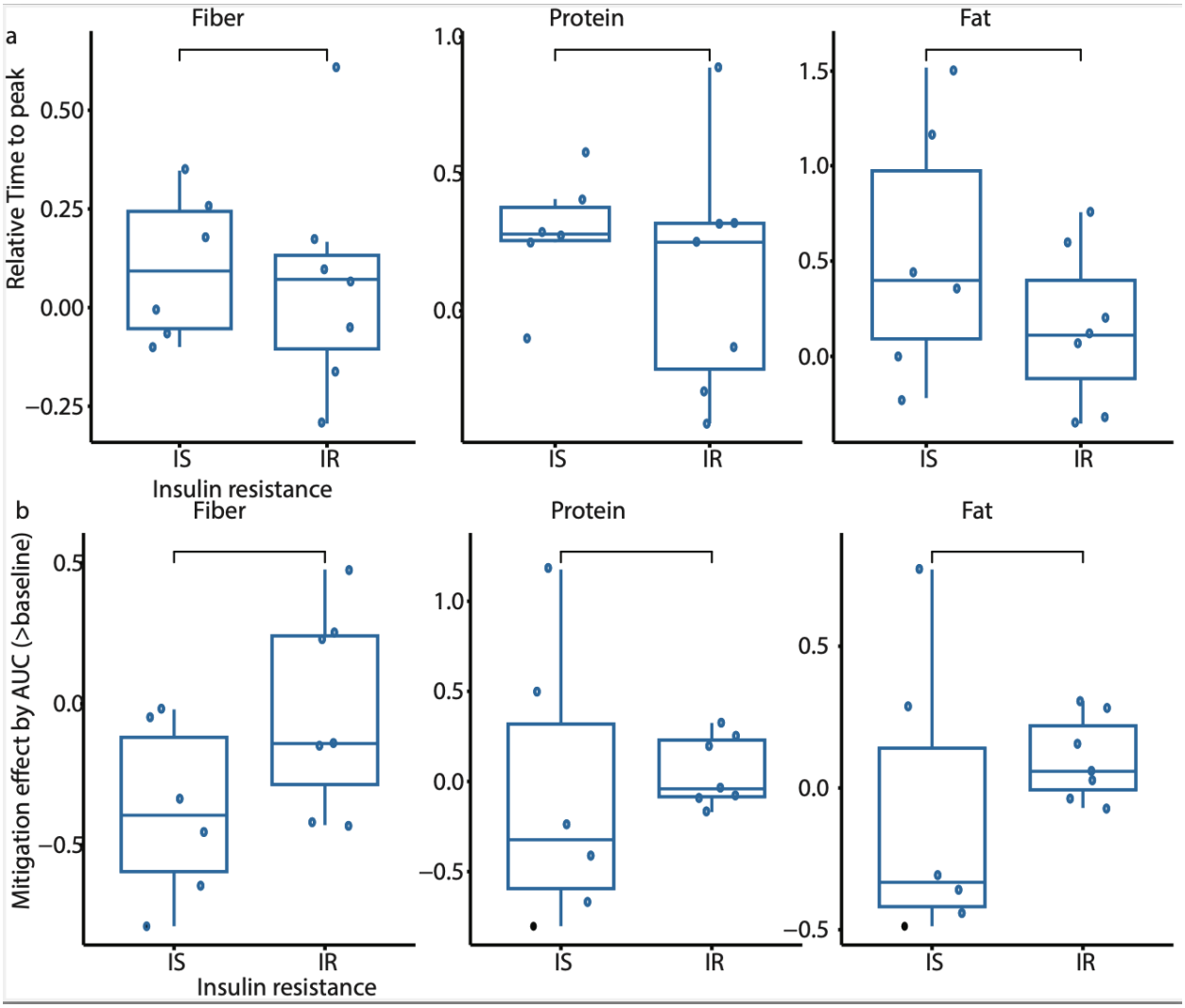

Figure S15: Differences in mitigation effects between IS and IR groups. a: Mitigation effect (ratio) between individuals who are insulin sensitive (IS) and insulin resistant (IR) classified by SSPG. Each figure is for one different mitigator and the boxplot shows mitigation effects for mitigator foods. The mitigation effect is the relative effect compared with the PPGR to only rice. Relative time to peak is the relative time difference with only rice. **b**: The mitigation effect by AUC (>baseline) is the relative AUC (>baseline) difference with only rice. The number of participants for IS (IR) is fiber 6 (7), protein 6 (7), and fat 6 (7). Extracted CGM features for each participant are compared between different metabolic subtypes. The boxplots show the center line as the median and the hinges as the 25th and 75th percentiles. The upper whisker extends from the hinge to the largest value not bigger than 1.5 times the distance between the hinges. Data beyond the whiskers are outliers.

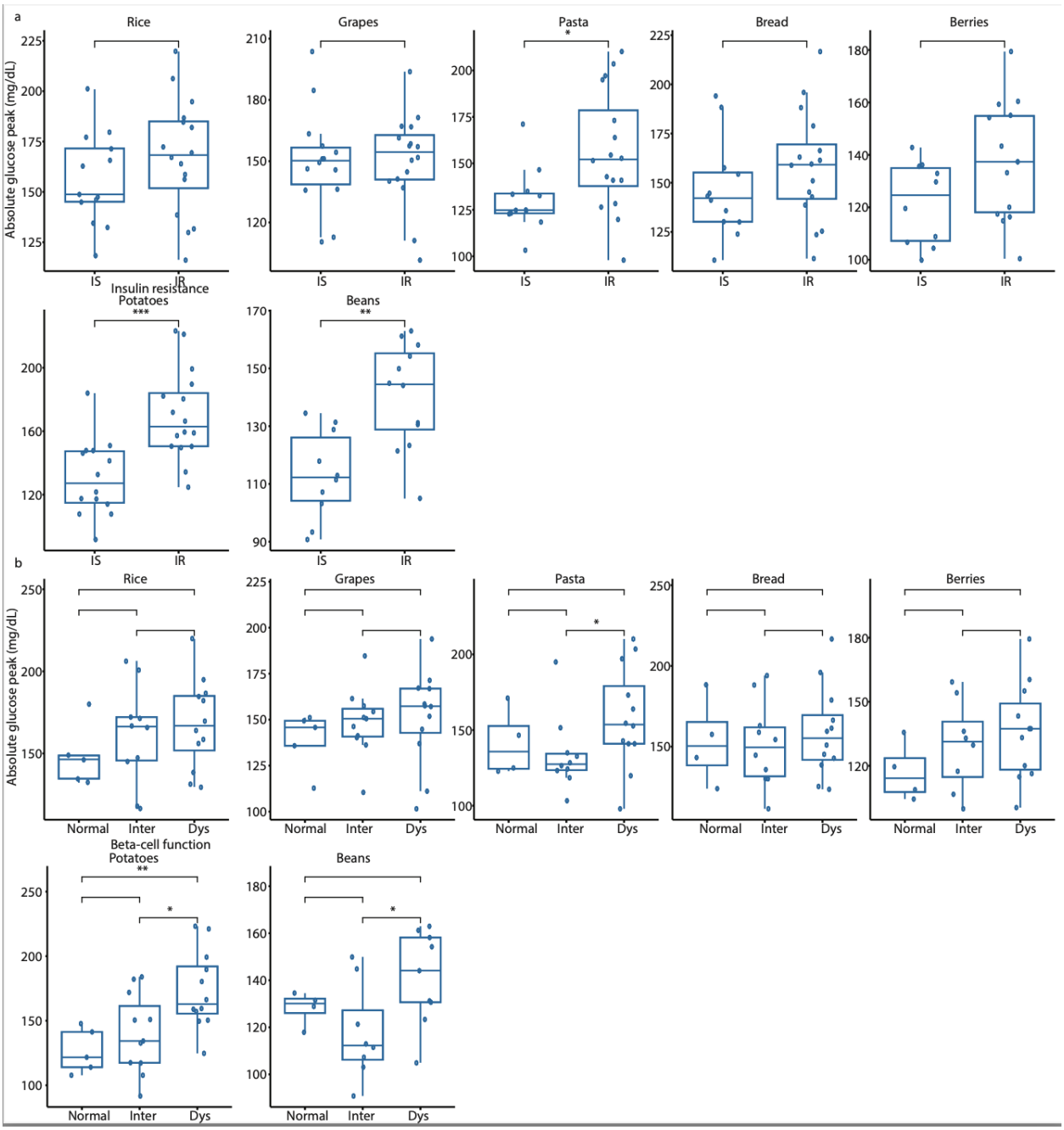

Figure S16: Comparison of absolute postprandial glycemic peaks between individuals with different levels of insulin resistance and beta cell function. a: Absolute glucose peak (mg/dL) between individuals who are insulin resistant (IR) and insulin sensitive (IS) measured by SSPG. Each figure is for one different meal and the boxplot shows the delta glucose peak for standardized carbohydrate meals. *: based on Holm corrected p-value of the Mann-Whitney test (two-sided, default) of selected pairs, *: p_H<=0.05, **: p_H<=0.01, ***: p_H<=0.001. The p_H is pasta 0.011, potatoes 1.5E-4, and beans 3.4E-3. **b**: Absolute glucose peak between individuals with normal, dysfunctional, and intermediate beta cell function. Beta cell function is quantified using DI which is adjusted by SSPG. The p_H is pasta inter vs dys 0.036, potatoes normal vs dys 1.3E-3, potatoes inter vs dys 0.032, and beans inter vs dys 0.036. The number of participants for IS (IR)

in a is rice 13 (16), grapes 14 (16), pasta 12 (16), bread 12 (16), berries 10 (14), potatoes 14 (16), and beans 10 (12). The number of participants for normal (intermediate, dysfunctional) beta cell function in b is rice 5 (10, 12), grapes 5 (11, 12), pasta 4 (10, 12), bread 4 (10, 12), berries 4 (8, 11), potatoes 5 (11, 12), and beans 4 (8, 9). Extracted CGM features for each participant are compared between different metabolic subtypes. The boxplots show the center line as the median and the hinges as the 25th and 75th percentiles. The upper whisker extends from the hinge to the largest value not bigger than 1.5 times the distance between the hinges. Data beyond the whiskers are outliers.

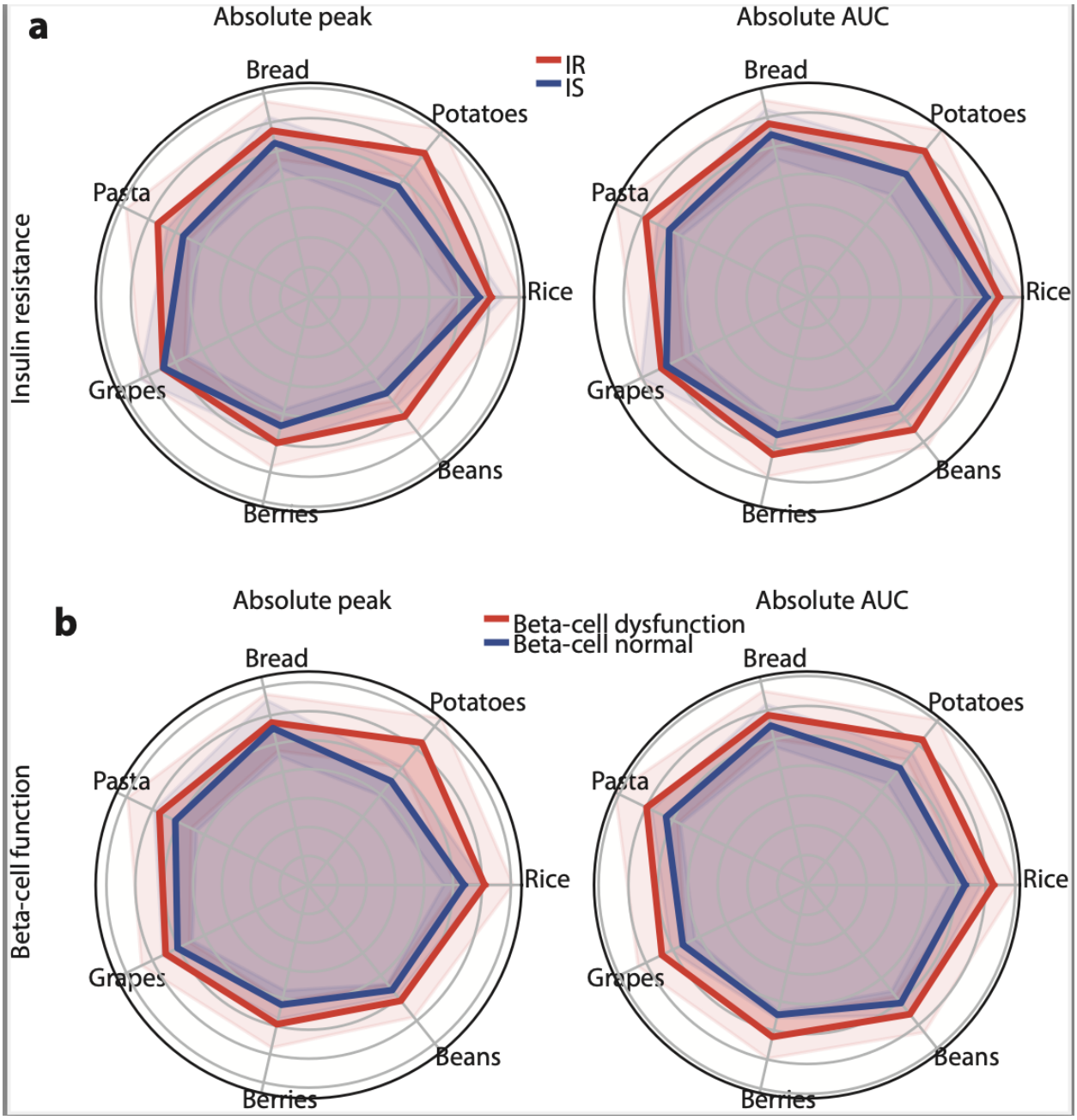

Figure S17: Differences in mean PPGRs between participants with different insulin resistance and beta cell function. **a** is the comparison of insulin resistant (IR) and insulin sensitive (IS) groups, and **b** is the comparison of normal and dysfunctional beta-cell groups. Each column is one type of quantification of PPGRs, including absolute peak intensity and absolute AUC. The solid line is the mean value, and the shade is one standard deviation. The number of participants for IS (IR) in a is rice 13 (16), grapes 14 (16), pasta 12 (16), bread 12 (16), berries 10 (14), potatoes 14 (16), and beans 10 (12). The number of participants for normal (dysfunctional) beta cell function in b is rice 5 (12), grapes 5 (12), pasta 4 (12), bread 4 (12), berries 4 (11), potatoes 5 (12), and beans 4 (9). Extracted CGM features for each participant are compared between different metabolic subtypes.

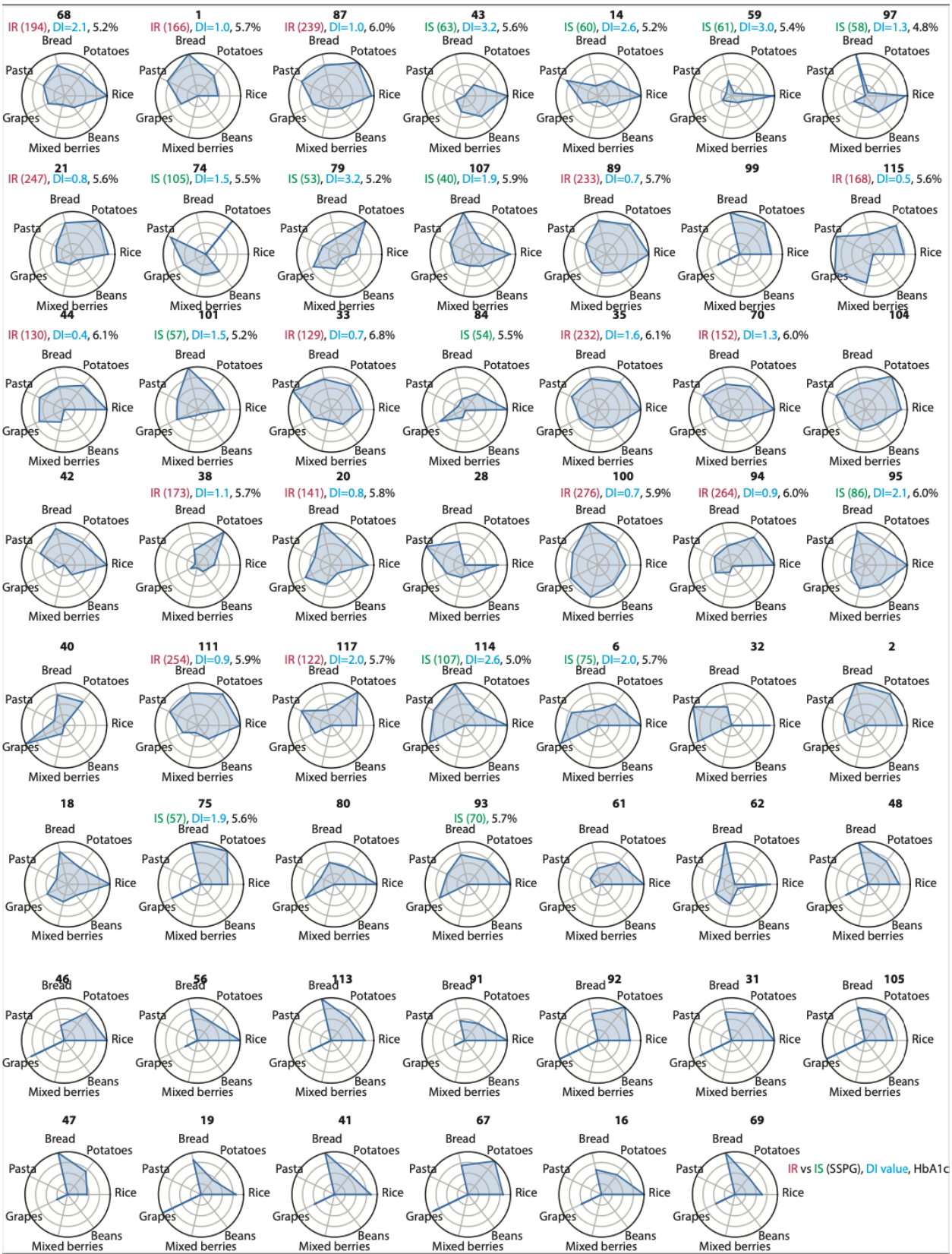

Figure S18: AUC (>baseline) of each meal in each participant. The value was averaged

among replicates and normalized by the maximum for that participant. Insulin resistance, SSPG, DI, and HbA1c were also presented.

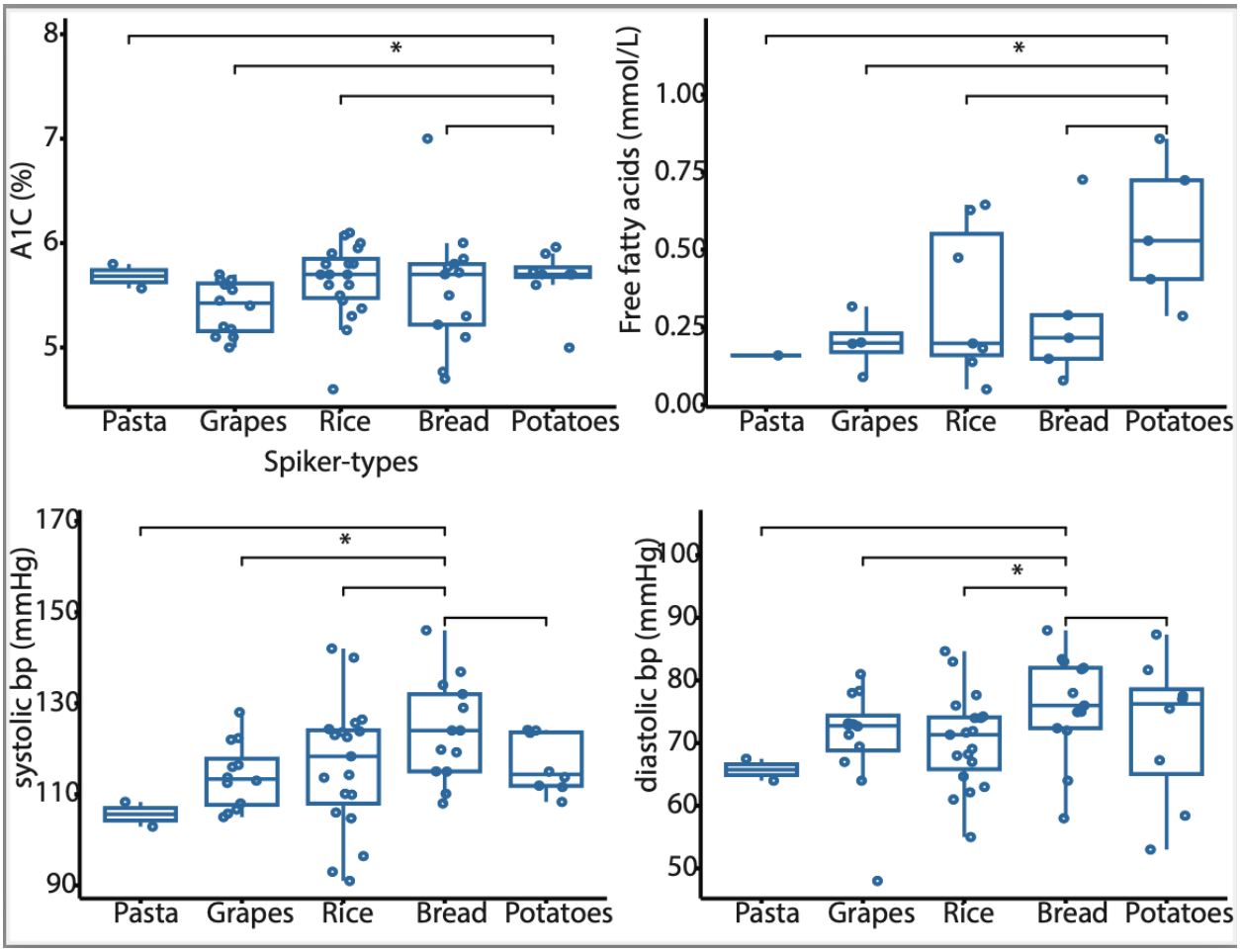

Figure S19: Clinical and metabolic characteristics according to carb-response-types. The x-axis is different carb-response-types. Horizontal lines between boxes indicate comparison and statistical significance is indicated by asterisks. Free fatty acids were measured during the first stage of the SSPG test (with insulin concentrations comparable to the non-fed state) reflecting adipocyte insulin resistance. Statistical comparisons utilized Holm corrected p-value of the Mann-Whitney test (default, two-sided) of the selected pairs, *: p_H<=0.05. The significant p_H from left to right top to bottom is 0.016, 0.032, 0.019, and 0.032. The number of participants for A1C (Free fatty acids, systolic bp, diastolic bp) is rice-spiker 19 (7, 19, 19), grape-spiker 12 (4, 12, 12), pasta-spiker 2 (1, 2, 2), bread-spiker 13 (5, 13, 13), and potato-spiker 8 (5, 8, 8). Clinical measurements were compared between carb-response-types. The boxplots show the center line as the median and the hinges as the 25th and 75th percentiles. The upper whisker extends from the hinge to the largest value not bigger than 1.5 times the distance between the hinges. Data beyond the whiskers are outliers.

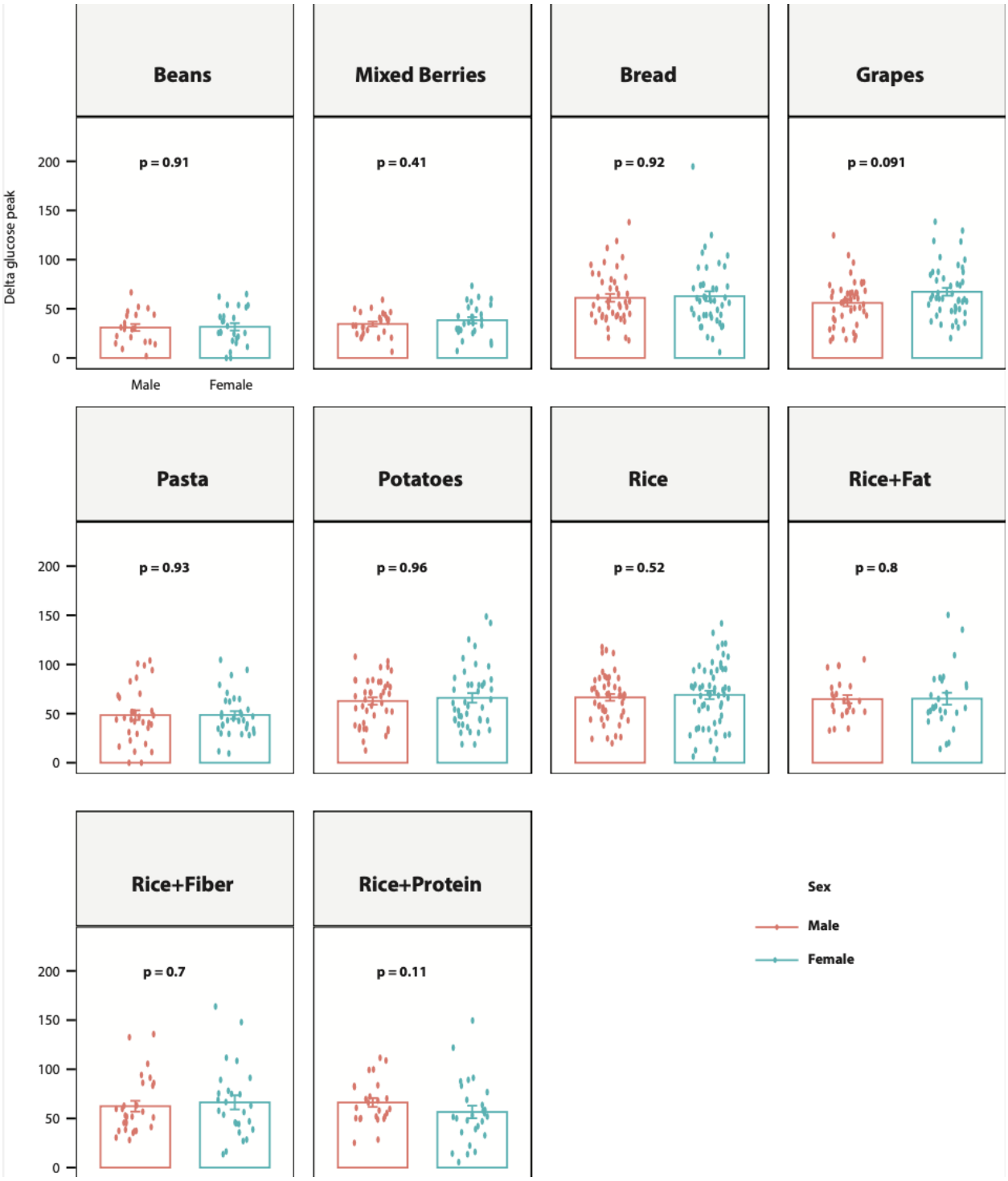

Figure S20: Differences in delta glucose peak between different sexes. Delta glucose peaks (mg/dL) were plotted between males and females. P-values were calculated based on the Mann-Whitney test (default, two-sided). The number of CGM curves (each dot) for female (male) is: rice 58 (49), potatoes 42 (41), bread 44 (45), pasta 32 (33), grapes 46 (46), beans 25 (21), mixed berries 27 (26), rice+fiber 26 (28), rice+protein 27 (25), and rice+fat 27 (24). Extracted CGM

features are compared between sex. Each participant was instructed to eat each meal at least twice at two different days.

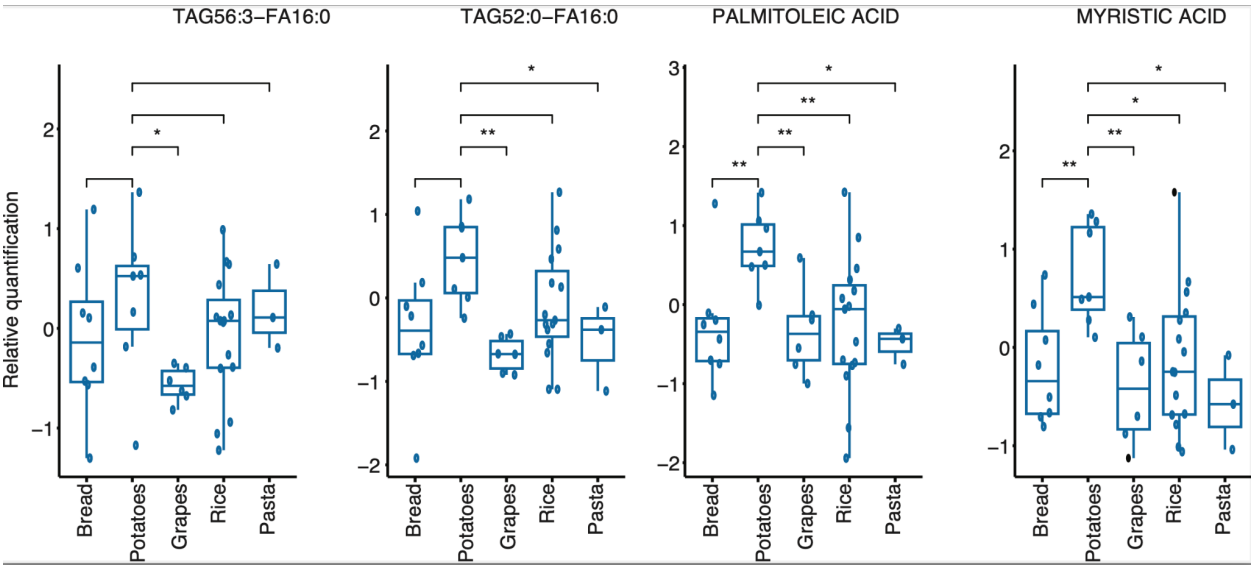

Figure S21: Metabolites and lipids that are distinguished between carb-response-types. The X-axes indicate different carb-response-types. Different metabolites are presented in different panels. *: based on Holm corrected p-value of the Mann-Whitney test (default, two-sided) of the selected pairs, *: p_H<=0.05, **: p_H<=0.01. The p_H is: grapes vs potatoes (left 1) 0.035, potatoes vs grapes (left 2) 1.2E-3, potatoes vs pasta (left 2) 0.033, potatoes vs bread (left 3) 9.3E-3, potatoes vs grapes (left 3) 8.2E-3, potatoes vs rice (left 3) 6.6E-3, potatoes vs pasta (left 3) 0.017, potatoes vs bread (right) 9.3E-3, potatoes vs grapes (right) 8.2E-3, potatoes vs rice (right) 0.014, and potatoes vs pasta (right) 0.017. The boxplots show the center line as the median and the hinges as the 25th and 75th percentiles. The upper whisker extends from the hinge to the largest value not bigger than 1.5 times the distance between the hinges. Data beyond the whiskers are outliers. The number of participants in each carb-response-types is rice-spiker (15), grape-spiker (6), pasta-spiker (3), bread-spiker (8), and potato-spiker (7). Omics measurements were compared between carb-response-types.